

INTRODUCTION

1.1 MOTIVATION

Missile guidance and control is a promising field of application for the latest developments in robust control theory. The sliding mode control technique is becoming popular in the flight control field because of its inherent insensitivity and robustness to plant uncertainties and external disturbances. This was the motivation behind using sliding mode control in this thesis for designing an autopilot system for a ballistic missile.

1.2 BALLISTIC MISSILE BASICS

The aerodynamic vehicle considered in this research work is a ballistic missile. Ballistic missiles have a ballistic trajectory over most of flight path. The missile is only guided during the relatively brief initial powered phase of flight and the laws of orbital mechanics and ballistics subsequently govern its course. Ballistic missiles are categorized according to their ranges, the maximum distance measured along the surface of the earth's ellipsoid from the point of launch of a ballistic missile to the point of impact [1].

Ballistic missiles are categorized according to their ranges as follows

- Intercontinental Ballistic Missile (ICBM) has range over 5500 kilometers.
- Intermediate-Range Ballistic Missile (IRBM) ranges from 3000 to 5500 kilometers.
- Medium-Range Ballistic Missile (MRBM) ranges from 1000 to 3000 kilometers.
- Short-Range Ballistic missile (SRBM) ranges up to 1000 kilometers.
- Strategic missile has range of over 1000 kilometers.
- Operational-Strategic missile ranges from 500 to 1000 kilometers.
- Operational missile ranges from 300 to 500 kilometers.
- Operational-Tactical missile ranges from 50 to 300 kilometers.
- Tactical missile has range up to 50 kilometers.

The trajectory of a ballistic missile consists of three phases

- The powered phase in which propellant is being burnt.
- The free-flight phase when no thrust is available, this phase constitutes major portion of the flight time.
- The re-entry phase when missile re-enters the Earth's atmosphere.

Ballistic missiles have a prescribed course that cannot be altered after the missile has burnt its fuel. A ballistic missile also follows a pre-established azimuth from launch point to the target.

1.2.1 MISSILE COMPONENTS

A Missile works on the principle of third Law of Motion, which states, "every action is accompanied by an equal and opposite reaction." The continuous ejection of a stream of hot gases in one direction causes a steady motion of the missile in the opposite direction. The major components of a missile assembly are a motor or engine, propellant consisting of fuel and an oxidizer, a frame to hold the components, control systems and a payload such as a warhead.

1.2.2 NAVIGATION SYSTEM

A "Navigation System" is one that automatically determines the position of the vehicle with respect to some reference frame, for example, the earth, and displays this to an operator to make the necessary correction.

1.2.3 GUIDANCE SYSTEM

A "Guidance System" on the other hand, automatically makes the necessary correction to keep the vehicle on course by sending the proper signal to the control system or autopilot. The guidance system then performs all the functions of a navigation system plus generating the required correcting signal to be sent to the control system. The type of guidance system to be used depends upon the type and mission of the missile being controlled, and it can vary in complexity from an inertial guidance system for long range surface to surface or air to surface winged missiles to a simple system where the operator visually observes the missile and sends guidance commands via a radio link.

1.2.4 CONTROL SYSTEM

The "Control System" controls the direction of the motion of the vehicle or simply the orientation of the velocity vector. A missile control system is also referred as "Missile Autopilot". The autopilot structure used in this work is based on Sliding Mode Control technique.

1.3 SCOPE OF THE WORK

The objective of this work is to present a robust autopilot structure for longitudinal dynamics of a missile via multiple-surface sliding mode control. The proposed control structure results in simple and flexible design with increased robustness as compared to already presented designs. The basic idea is to minimize the normal position and velocity deviations (guidance errors) when a trajectory following guidance is employed. The proposed controller assumes a completely uncertain statically stable plant dynamics in pitch plane and the control law is just based on sliding mode rate reaching laws ensuring the stability of the system via Lyapunov direct method. SMC practical implementation will also be discussed. The proposed control strategy is applied to a tail controlled ballistic missile system in pitch plane. Static stability of the plant is analyzed by considering the linear time invariant dynamics of the missile system in frequency domain and is ensured by making all the poles of plant to remain in the left half of imaginary axis during the total flight regime. The coupled nonlinear three dimensional missile dynamics is also presented. The performance of the overall nonlinear control system is analyzed in the presence of environmental disturbances using a Nonlinear/Six DOF simulator. The linear system dynamics is also compared with Nonlinear SixDOF Simulator dynamics. System robustness analysis is also performed using SixDOF (Six Degrees of Freedom) simulations. Simulation results show that the proposed algorithm is able to give good performance regardless of the uncertainties and time varying disturbances.

1.4 CHAPTERS ORGANISATION

The brief description of each chapter is given below:

Chapter 2 is about the literature review of the work done in the related field.

In chapter 3 we briefly discuss over all dynamic system components and guidance scheme used for the system design. Linear System dynamics is also presented for a tail controlled ballistic missile System.

In chapter 4 proposed control strategy based on multiple surface sliding mode control for a hypothetical ballistic missile system is discussed while giving its benefits and limitations.

In chapter 5 closed loop system performance is discussed, using SixDOF/Nonlinear simulation in the presence of environmental disturbances. System is checked for robustness against parameter

variations. The Linear system dynamics presented in chapter 3 is also validated on Nonlinear SixDOF simulator.

In chapter 6 conclusion and future work is discussed.

LITERATURE REVIEW**2.1 INTRODUCTION**

In this chapter the literature review of the work done in the related field is discussed. Though many research papers and books were consulted which are included in the references, but here few research papers will be discussed briefly.

2.2 BRIEF STUDY UNDERTAKEN

The fundamental purpose of autopilot design for missile systems is to provide satisfactory stability, performance and robustness over a wide range of flight conditions in which their aerodynamic coefficients vary over a wide dynamic range due to large Mach-altitude fluctuations and due to aerodynamic coefficient uncertainties resulting from inaccurate wind-tunnel measurements [2].

Missile autopilots are usually designed to track acceleration commanded by a guidance law on the basis of data sensed and estimated by a navigation system, where a widely accepted approach is to estimate relative position, velocity and acceleration via extended Kalman Filtering Technique [2].

While designing a controller for a nonlinear flight vehicle it is common practice to represent the flight envelope by a grid of Mach-altitude operating points and then linearization of the nonlinear state equations is performed at trim points of the gridded flight envelope. The plant in fact becomes a differential inclusion under continuously varying flight conditions. Several possible design techniques have been presented for dealing with such control problems. The classical approach is to design a controller for a certain point and then to schedule the controller's gain to place eigen values deep in the left side of the imaginary axis and the near real-axis according to a measured or derived parameters that represent flight conditions, such as angle of attack or Mach number [3], [4].

In another approach, H_∞ methods are invoked to design a collection of controllers, where, for each operating point in the flight envelope grid, a controller with a fixed structure results [5]. The ensuing set of controllers is then transformed to a single gain scheduled controller by obtaining a

least square fit of its parameters with respect to angle of attack, or Mach number, and so forth. For highly agile air vehicles, these techniques would result in an extensive number of controller design points to be able to cope with the drastically changing dynamic behavior throughout the flight envelop. All of the aforementioned methods are linear design techniques that require either exact knowledge of system parameters or, alternatively, assumption of some uncertainty model such as norm boundedness, thus allowing for robust controller design.

Various nonlinear control approaches have been investigated in the research literature, in [6], [7] two approaches to nonlinear robust control design are examined, the first approach uses an inner loop to linearize the plant from input /output sense using dynamic inversion method. The second approach examined in this paper, uses a recursive, or back stepping design procedure to derive a nonlinear controller. In [8], a new robust nonlinear controller structure using feedback linearization technique is presented. It linearizes the nonlinear dynamics, decouples the longitudinal and lateral motions and caters the model uncertainty.

A robust adaptive optimal tracking control design for missile systems with unknown (or uncertain) parameters and external disturbance based on adaptive fuzzy technique is proposed in [9]. An adaptive fuzzy control is equipped with an optimal robust control to achieve the desired tracking performance for uncertain missile systems with external disturbance. The design procedure is divided into two steps. First, a fuzzy-based adaptive feedback linearization control scheme is designed to achieve the tracking of unknown (or uncertain) missile systems. Next, a combined optimal robust control scheme is employed to minimize the worst-case effect arising from adaptive fuzzy approximation error and external disturbance to improve the tracking performance of missile. Although many other nonlinear techniques have been presented in the research literature but this research focuses on Sliding Mode Control which would be discussed in rest of the thesis.

2.2.1 ADVANCED MISSILE AUTOPILOT REQUIREMENTS

The following characteristics for missile autopilot are of practical interest [2]:

- A simple clear structure, which can be readily designed, facilitated, implemented, tuned up and monitored.
- Increase both performance and robustness to disturbances and system parametric uncertainties.

- The least possible modeling information to guarantee these performance and robustness.
- Relax the sensor/processor/actuator requirements without introducing new restrictive assumptions, which are difficult to verify.
- Have maximum autonomy with respect to common sensed data so that it can be easily integrated with different navigation/ guidance systems.
- Have the provision that a professional with common relevant control theory background can easily conduct on-the-fly ad hoc inevitable modifications.

Almost all the above-mentioned characteristics are fulfilled by Sliding Mode Control (SMC) systems.

2.2.2 SLIDING MODE CONTROL IN MISSILE GUIDANCE & CONTROL

The Sliding Mode Control technique is becoming popular in the flight control field because of its inherent insensitivity and robustness to plant uncertainties and external disturbances [2]. In addition, a new generation of sliding mode algorithms (high order sliding modes) featuring usually 1st or 2nd order dynamics in traditional static nonlinear state feedback (conventional sliding mode), produces continuous control input, which can explicitly account for not only actuator saturation but also rate saturation limit. The other additional features include enhanced robustness to measurement noise and opportunity to realize output feedback instead of full state feedback to increase robustness to parametric and dynamic uncertainties.

Sliding mode design based on Lyapunov matrices is also proposed as roll autopilot for tail-controlled missile [10]. SMC combined with optimizing techniques gives additional benefit of optimization while achieving robustness. This methodology has been extended to linear time varying (LTV) systems and applied to lateral autopilot design in [11]. In [12], SMC is used for design of missile guidance law, which is robust to target maneuvers and hence compares better in terms of performance with existing guidance laws. The latest trend in designing missile flight control systems is to combine the outer loop guidance design, with the inner loop autopilot design [13]. Such an integrated design is compared with classical approach of two-loop case for rapid maneuvers and advantages of integrated approach have been demonstrated. An enhanced sliding mode controller based on nonlinear disturbance observer is also proposed for longitudinal dynamics of a highly maneuverable missile in [14].

Various complex hybrid sliding mode controller structures also have been proposed. These hybrid controllers try to ensure the asymptotical stability and to reduce the chattering by combining the sliding mode control with other techniques, such as adaptive control techniques and Fuzzy control techniques. Most of these hybrid controllers require complex implementation algorithms. A sliding mode controller with on line neural net control is developed to ensure the system robustness against the uncertainties [15]. In [16] the concept of multiple surfaces sliding control has been proposed for pneumatic servo system, here we extend this concept to missile guidance and control.

2.3 SUMMARY

In this chapter a brief overview of the research work done in the field of autopilot design for aerodynamic vehicle was discussed. In this work we focus on Sliding mode control to design an autopilot system for longitudinal dynamics of a tail controlled ballistic missile system. Similar approach may be used for lateral dynamics of the system as well. A brief description of overall system is given in next chapter.

SYSTEM DESCRIPTION

3.1 INTRODUCTION

The objective of the thesis is to design Autopilot for an aerodynamic vehicle to implement the steering commands obtained from the guidance loop and to ensure a stable flight under the presence of environmental disturbances. The aerodynamic vehicle considered in this thesis is a ballistic missile whose dynamics are continuously changing due to changing aerodynamic coefficients due to the mach altitude fluctuation throughout the flight. In this chapter we define the overall block diagram of the closed loop control system and briefly discuss the dynamics of each block.

3.2 BLOCK DIAGRAM

The block diagram of the flight control system is as shown in Fig 3.1 below.

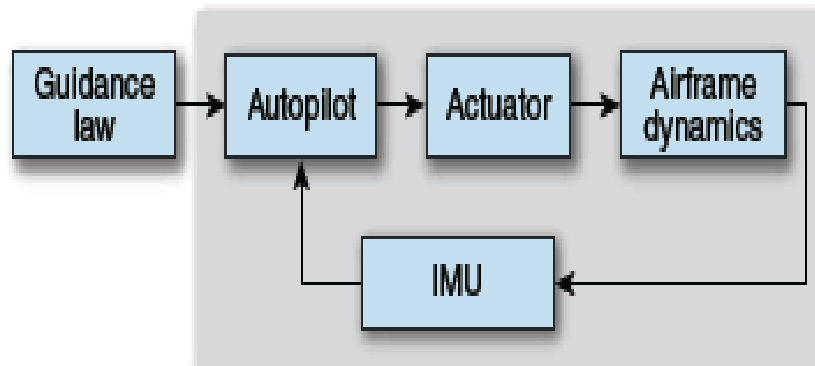


Fig. 3.1 Block Diagram of Flight Control System

An Inertial Measurement Unit (IMU) measures the missile translational acceleration and angular velocity. The outputs of the IMU are combined with the guidance commands in the autopilot to compute the commanded control input, such as a desired tail-surface deflection or thrust-vector angle. An actuator (usually an electromechanical system), forces the physical control input to follow the commanded control input. The airframe dynamics respond to the control input. The basic objective of the flight control system is to force the achieved missile dynamics to track the

guidance commands in a well-controlled manner. Here we provide an overview of each element of the flight control loop [17] - [19].

3.3 GUIDANCE SCHEME

Trajectory following guidance scheme is used in this research. The main objective of the guidance scheme is to follow a pre-determined path to remove the range error due to any type of disturbance.

3.4 AIRFRAME DYNAMICS

Recall that the objective of the flight control system is to force the missile dynamics to track the input command. The dynamics of the airframe are governed by fundamental equations of motion, with their specific characteristics determined by the missile aerodynamic response, propulsion, and mass properties. Assuming that missile motion is restricted to the vertical plane (typical for early concept development), the equations of motion that govern the missile dynamics can be developed in straightforward fashion.

Consider the diagram in Fig. 3.2, which shows the missile flying in space constrained to the vertical plane.

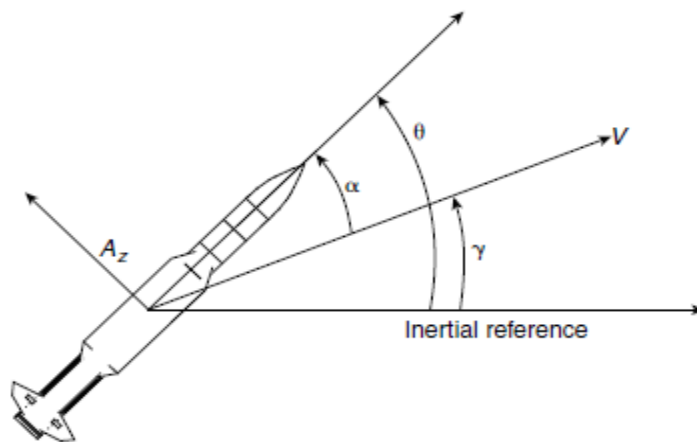


Fig. 3.2 Missile Dynamic Variables

The angle between the inertial reference axis and the missile velocity vector is called the flight-path angle “ γ ”. The angle from the velocity vector to the missile centerline is called the angle of attack (AOA) “ α ”. The angle from the inertial reference to the missile centerline is called the

pitch angle “ θ ”. Acceleration in the direction normal to the missile “ A_N ” derives from two sources. The non-zero AOA generates aerodynamic lift. Normal acceleration can also be developed by a control input “ δ ” such as tail-fin deflection or thrust-deflection angle. In general, the missile acceleration also has a component along the centerline due to thrust and drag. For the simple model being developed here, we assume that this acceleration is negligible. Based on the diagram in Fig. 3.2, the fundamental relationship among the three angles above is [17] - [19].

$$\alpha = \theta - \gamma \rightarrow \dot{\alpha} = \dot{\theta} - \dot{\gamma} \quad 3.5$$

The angular acceleration is the moment applied to the airframe divided by the moment of inertia, the applied moment is a function of the control input δ and the aerodynamic force induced by the AOA [17].

$$\dot{q} = \frac{M \alpha, \delta}{J} \quad 3.6$$

where,

$q = \dot{\theta}$	Pitch Rate
$\dot{q} = \ddot{\theta}$	Pitch Angular Acceleration
M	Applied Pitch Moment
J	Body Inertia
δ	Control Fin Deflection
α	Angle of Attack

The rate of change of the flight-path angle is the component of missile acceleration perpendicular to the velocity vector divided by the magnitude of the velocity vector. Assuming that the AOA is small, the flight-path angle rate is

$$\dot{\gamma} = \frac{A_N \cos(\alpha)}{V} \approx \frac{A_N}{V} \quad 3.7$$

The normal acceleration is determined by the forces applied to the missile divided by its mass [17],

$$A_N = \frac{F_Z(\alpha, \delta)}{m} \quad 3.8$$

where,

$$\begin{aligned} V & \text{ Vehicle Velocity} \\ F_Z & \text{ Applied Force Around Z-axis} \\ m & \text{ Body Mass} \end{aligned}$$

The applied force is a function of the control input “ δ ” and the aerodynamic force induced by the AOA. Substituting Eq. 3.7 and Eq. 3.8 and combining the result with Eq. 3.6 and 3.5 yields a coupled set of nonlinear differential equations where the state variables are the AOA and the pitch rate [17] - [19].

$$\dot{\alpha} = q - \frac{F_Z(\alpha, \delta)}{mV} \quad 3.9$$

$$\dot{q} = \frac{M}{J} \alpha, \delta \quad 3.10$$

In reality, missiles are not constrained to motion in a single plane. Fig. 3.3 shows the relevant variables that describe the missile kinematics in three dimensions. The angle of sideslip (AOS) “ β ” is the yaw equivalent to the AOA. Together, they completely specify how the missile body is oriented relative to its velocity vector. The three components of the missile body angular velocity vector resolved in body-fixed coordinates are denoted p , q , and r , denoting the roll, pitch, and yaw rate, respectively. Applying the Newton–Euler equations of motion, can develop the equations that govern the dynamics of the missile. The translational motion can be described in terms of the derivatives of the AOA and the AOS. The rotational motion can be described in terms of the angular accelerations and takes a simple form assuming that products of inertia are zero. Figure 3.3 defines quantities used to describe the three-dimensional missile kinematics. Two angles are used to orient the missile relative to the velocity vector, either AOA and AOS or total AOA and aerodynamic roll angle. The components of the missile inertial velocity vector resolved in body-fixed axes are V_Z , V_Y , and V_X (not shown). The components of the inertial angular velocity vector resolved in body-fixed coordinates are p , q , and r . The coupled Nonlinear dynamics of the missile system may be represented as [17] - [19].

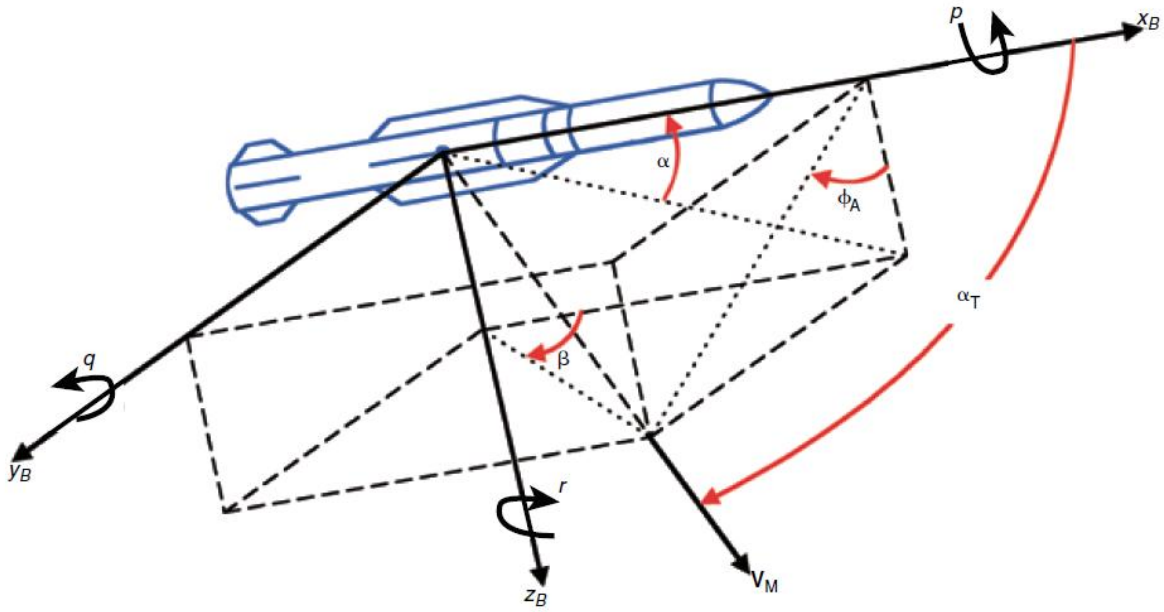


Fig. 3.3 Three dimensional missile kinematics

$$\begin{aligned} \dot{\alpha} &= \text{Cos}^2 \alpha \left\{ -\frac{F_{zb}}{mV_Z} - p \tan \beta + q \sec^2 \alpha - \frac{F_{xb}}{mV_Z} \tan \alpha - r \tan \alpha \tan \beta \right\} \\ \dot{\beta} &= \text{Cos}^2 \beta \left\{ \frac{-F_{yb}}{mV_Y} - r \sec^2 \beta + p \tan \alpha - \frac{F_{xb}}{mV_Y} \tan \beta + q \tan \alpha \tan \beta \right\} \end{aligned} \quad 3.11$$

$$\begin{aligned} \dot{p} &= \frac{M_{xb}}{J_x} - \frac{J_z - J_y}{J_x} qr \\ \dot{q} &= \frac{M_{yb}}{J_y} - \frac{J_x - J_z}{J_y} pr \\ \dot{r} &= \frac{M_{zb}}{J_z} - \frac{J_y - J_x}{J_z} pq \end{aligned} \quad 3.12$$

The lateral components of missile inertial translational acceleration resolved in body-fixed

Coordinates are

$$\begin{aligned}
A_N &= \frac{F_{zb}}{m} \\
A_y &= \frac{F_{yb}}{m}
\end{aligned}
\tag{3.13}$$

where,

β	Angle of side slip
p	Body roll rate
q	Body pitch rate
r	Body yaw rate
V_Y, V_Z	Missile Velocity components
J_x, J_y, J_z	Missile Inertia components
M_{xb}, M_{yb}, M_{zb}	Moment components
F_{zb}, F_{yb}	Force components
A_N, A_y	Acceleration components

In these equations the forces and moments are resolved in body coordinates, with components indicated by the subscripts. Though not shown explicitly, all of the six components of the force and moment vectors are functions of the state variables and three control inputs, e.g.,

$$F_b = f(\alpha, \beta, p, q, r, \delta_p, \delta_y, \delta_r) \tag{3.14}$$

The dynamic equations together are a coupled, fifth-order, nonlinear differential equation. In situations where the mass properties vary with time, such as when a rocket motor is burning propellant, the differential equation is time varying as well. Eq.3.11- Eq.3.14 can be linearized (Linearization of only pitch plane dynamics will be presented in next section) around some operating condition of interest by expanding them in a Taylor series and retaining only the first-order terms. The result is a linear, time-invariant, state-space model with three inputs and five

outputs [17] – [19].

$$\begin{aligned}
 \dot{x} &= Ax + Bu \\
 y &= Cx + Du \\
 x &= [\alpha \ \beta \ p \ q \ r] \\
 u &= [\delta_p \ \delta_q \ \delta_r]^T \\
 y &= [A_y \ A_z \ p \ q \ r]^T
 \end{aligned} \tag{3.15}$$

As in the planar case, the state variables, control input variables, and output variables represent perturbations around the nominal operating condition. Expanding the model to account for yaw and roll in addition to pitch brings a new set of challenges to the flight control designer. Foremost among these in many applications is aerodynamic cross-coupling as the total AOA increases, resulting in aerodynamic imbalances. The net effect typically results in undesirable motion, such as roll moment induced by a change in AOA or pitch moment induced by roll control input. The flight control system must compensate for these effects. An alternative is to simplify the airframe design to minimize cross-coupling, but the airframe must be designed with other factors in mind as well, such as maximizing the effective range of the missile. Compensating for aerodynamic cross coupling for some missiles is challenging and often limits the maximum total AOA, and hence the maximum lateral acceleration, that can be achieved by the flight control system.

3.4.1 Dynamics Linearization

Here Linearization is restricted to pitch plane only since our aim is to fully understand and design an autopilot for longitudinal dynamics of the system. Recall from Sec 3.4 the coupled nonlinear differential dynamic equations in pitch plane are given as [17] – [19],

$$\begin{aligned}
 \dot{\alpha} &= \cos^2 \alpha \left\{ \frac{-F_{zb}(\alpha, \delta)}{mV} - p \tan \beta + q \sec^2 \alpha - \frac{F_{xb}(\alpha, \delta)}{mV} \tan \alpha - r \tan \alpha \tan \beta \right\} \\
 \dot{q} &= \frac{M_{yb}}{J_y} - \frac{J_x - J_z}{J_y} pr \\
 A_N &= \frac{F_{Zb}(\alpha, \delta)}{m}
 \end{aligned} \tag{3.16}$$

The equations of motion are linearized around an operating condition so that linear systems theory can be applied. Assuming zero coupling between different axis dynamics, constant missile speed and, $\alpha \cong 0$, linearization of above equation yields a second-order state-space description of the missile dynamics. Since we know that

$$\dot{x} = \left(\frac{\partial f}{\partial x} \right)_{x=0, u=0} x + \left(\frac{\partial f}{\partial u} \right)_{x=0, u=0} u + f_{h.o.t}$$

Then,

$$\begin{aligned} \dot{\alpha} &= \left\{ -\frac{1}{mV} \frac{\partial}{\partial \alpha} F_{zb}(\alpha, \delta) \alpha - \frac{1}{mV} \frac{\partial}{\partial \delta} F_{zb}(\alpha, \delta) \delta + q \right\} \\ \dot{q} &= \frac{1}{J_y} \frac{\partial}{\partial \alpha} M_{zb}(\alpha, \delta) \alpha + \frac{1}{J_y} \frac{\partial}{\partial \delta} M_{zb}(\alpha, \delta) \delta \\ A_N &= \frac{1}{m} \frac{\partial}{\partial \alpha} F_{zb}(\alpha, \delta) \alpha + \frac{1}{m} \frac{\partial}{\partial \delta} F_{zb}(\alpha, \delta) \delta \end{aligned} \quad 3.17$$

Where the numerical coefficients are defined by

$$\begin{aligned} Z_\alpha &= \frac{1}{m} \frac{\partial F_z(\alpha, \delta)}{\partial \alpha} \\ Z_\delta &= \frac{1}{m} \frac{\partial F_z(\alpha, \delta)}{\partial \delta} \\ M_\alpha &= \frac{1}{J_z} \frac{\partial M_z(\alpha, \delta)}{\partial \alpha} \\ M_\delta &= \frac{1}{J_z} \frac{\partial M_z(\alpha, \delta)}{\partial \delta} \end{aligned} \quad 3.18$$

where,

- α Angle of attack
- q Pitch rate
- δ The control surface deflection
- M_δ Pitch control derivative
- M_α Pitch moment derivative
- Z_α Lift force slope derivative
- Z_δ Lift force control derivative

The simplification results in

$$\begin{aligned} \begin{bmatrix} \dot{\alpha} \\ \dot{q} \end{bmatrix} &= \begin{pmatrix} \frac{-Z_\alpha}{V} & 1 \\ M_\alpha & 0 \end{pmatrix} \begin{bmatrix} \alpha \\ q \end{bmatrix} + \begin{bmatrix} \frac{-Z_\delta}{V} \\ M_\delta \end{bmatrix} \delta \\ \begin{bmatrix} q \\ A_N \end{bmatrix} &= \begin{pmatrix} 0 & 1 \\ Z_\alpha & 0 \end{pmatrix} \begin{bmatrix} \alpha \\ q \end{bmatrix} + \begin{bmatrix} 0 \\ Z_\delta \end{bmatrix} \delta, \end{aligned} \tag{3.19}$$

where,

$$\begin{aligned} A &= \begin{pmatrix} \frac{-Z_\alpha}{V} & 1 \\ M_\alpha & 0 \end{pmatrix}, B = \begin{bmatrix} \frac{-Z_\delta}{V} \\ M_\delta \end{bmatrix} \\ C &= \begin{pmatrix} 0 & 1 \\ Z_\alpha & 0 \end{pmatrix}, D = \begin{bmatrix} 0 \\ Z_\delta \end{bmatrix}, u = \delta \end{aligned}$$

Because these differential equations result from linearization around an operating point, the state, input, and output variables actually represent small signal perturbations around that operating point. These linear differential equations apply for any missile under the stated assumptions. However, specific dynamics governed by these equations differ depending on the application. The linear differential equations determine the dynamic behavior of the missile for small perturbations around the specified operating conditions. For example, suppose the missile is given an initial condition at an AOA a few degrees away from the nominal AOA around which the dynamics have been linearized. One important question is whether the missile will rotate back to the nominal AOA or diverge in the absence of any corrective control input. The answer to this question of stability is determined by the roots of the characteristic polynomial of the state matrix in Eq. 3.19. The state-space representation in this equation describes the missile dynamics in the time domain. A representation in the complex frequency domain can be obtained that relates the input to the system, e.g., tail-deflection angle, to the system outputs, e.g., pitch rate and normal acceleration. This type of representation is called the transfer function and can be determined from the state-space model using the formula,

$$H(s) = C(sI - A)^{-1}B + D \tag{3.20}$$

Where $s = \sigma + j\omega$ is complex frequency and $A, B, C,$ and D are defined in Eq. 3.19, The system

transfer function from δ to A_N is to be given by

$$\frac{A_N}{\delta} = \frac{Z_\delta s^2 + Z_\alpha M_\delta - Z_\delta M_\alpha}{s^2 + \frac{Z_\alpha}{V} s - M_\alpha} \quad 3.21$$

The characteristic equation of the system transfer function is to be given by

$$s^2 + \frac{Z_\alpha}{V} s + (-M_\alpha) = 0 \quad 3.22$$

A necessary and sufficient condition for both roots of this equation to have negative real parts and thus ensure stability is that all of the coefficients be positive. Using the conventions in Fig. 3.3 Z_α is always positive. Therefore, the stability of the missile in the absence of a control input is determined by the sign of M_α .

If M_α is positive, the aerodynamic pitching moment forces the missile to diverge from the nominal AOA, and the missile is said to be statically unstable. If M_α is negative, the missile tends to be restored back to the nominal AOA, and the missile is said to be statically stable. The static stability of the missile is a crucial property that, under the stated assumptions, is determined solely by the sign of M_α , which is in turn determined by the aerodynamic configuration and the location of the missile center of mass.

Fig. 3.4 illustrates the open loop pole zero plot for the plant dynamics (see Appendix B) for $t=0$ sec.

$$\frac{A_N}{\delta} = \frac{109s^2 - 26288}{s^2 + 0.323s + 87.66} \quad 3.23$$

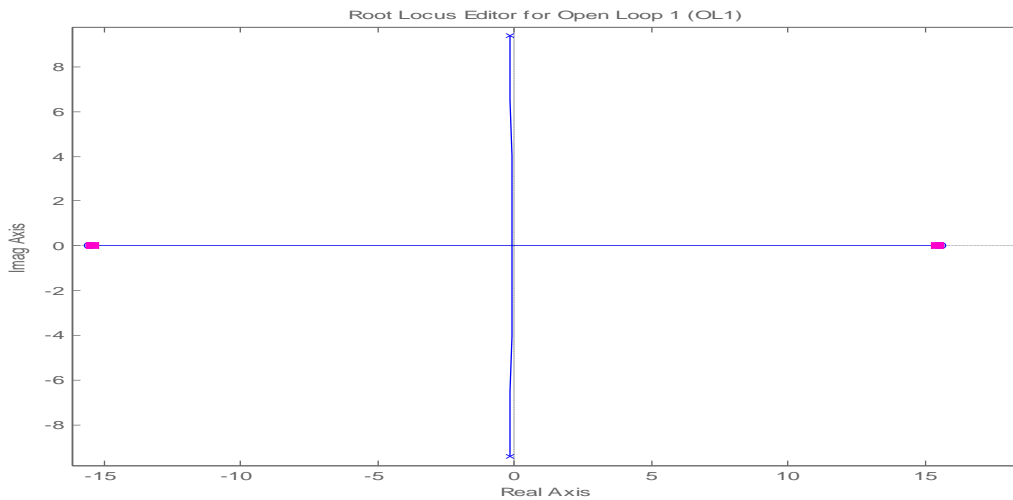


Fig. 3.4 PZ Map for Open Loop Transfer Function

3.5 ACTUATOR

The missile actuator converts the desired control command developed by the autopilot into physical motion, such as rotation of a tail fin, which will affect the desired missile motion. Actuators for endo-atmospheric missiles typically need to be high-bandwidth devices (significantly higher than the desired bandwidth of the flight control loop itself) that can overcome significant loads. Most actuators are electromechanical, with hydraulic actuators being an option in certain applications. For early design and analysis, the actuator dynamics are modeled with a second-order transfer function (which does not do justice to the actual complexity of the underlying hardware), although the actuator often is modeled as a linear system for preliminary design and development, it is actually a nonlinear device, and care must be taken by the flight control designer not to exceed the hardware capabilities. Two critical FOMs (Figures Of Merits) for the actuator for many endo-atmospheric missiles are its rate and position limits. The position limit is an effective limit on the moment that the control input can impart on the airframe, which in turn limits the maximum AOA and acceleration. The rate limit essentially limits how fast the actuator can cause the missile to rotate, which effectively limits how fast the flight control system can respond to changes in the guidance command. The performance of a flight control system that commands the actuator to exceed its limits can be degraded, particularly if the missile is flying at a condition where it is statically unstable.

The actuator used in this research is a servo system and is employed to give precise & accurate deflection to fins. There are four actuators which are connected to four fins. Command from controller is passed through a resolver whose function is to resolve the control command for four fins. The actuator is a self contained closed loop system consisting of three phase brushless dc motor, power amplifiers, transistors and Hall sensors whose dynamics was estimated by System Identification technique which may be represented as [20],

$$\frac{\delta_c}{\delta} = \frac{957.9s + 7900}{s^3 + 54.23s^2 + 957.9s + 7900} \quad 3.24$$

Where, δ_c is the command given to the system by the actuator.

3.6 INERTIAL MEASUREMENT UNIT (IMU)

The IMU measures the missile dynamics for feedback to the autopilot. In most flight control applications, the IMU is composed of accelerometers and gyroscopes to measure three

components of the missile translational acceleration and three components of missile angular velocity. For each rate and acceleration channel, like the actuator, the IMU needs to be a high-bandwidth device relative to the desired bandwidth of the flight control loop. In some applications, other quantities also need to be measured, such as the pitch angle for an attitude control system. In this case, other sensors can be used (e.g., an inertial stabilized platform), or IMU outputs can feed navigation equations that are implemented in a digital computer to determine the missile attitude, which then is sent to the autopilot as a feedback measurement. The flight control system must be designed such that the missile dynamics do not exceed the dynamic range of the IMU. If the IMU saturates, the missile will lose its inertial reference, and the flight control feedback is corrupted. The former may be crucial, depending on the specific missile application and the phase of flight, latter may be more problematic if the dynamic range is exceeded for too long, particularly if the missile is statically unstable. The transfer function of the IMU was approximated as a first order lag, since a delay of 130msec was given in IMU specification, thus

$$G_s = \frac{1}{0.13s + 1} \quad 3.25$$

3.7 AUTOPILOT

The autopilot is a set of equations that takes as inputs the guidance commands and the feedback measurements from the IMU and computes the control command as the output. As mentioned previously, the autopilot must be designed so that the control command does not cause oversaturation of the actuator or the IMU. Because the autopilot usually is a set of differential equations, computing its output involves integrating signals with respect to time. Most modern autopilots are implemented in discrete time on digital computers, although analog autopilots are still used.

3.8 SUMMARY

In this chapter we have discussed overall system block diagram and briefly explained each block. We have discussed the plant (airframe dynamics), especially the dynamics of the plant in pitch channel. The dynamics linearization was also presented. The static stability of linear system was analyzed in frequency domain. Figures of merits of each block were also discussed.

ROBUST AUTOPILOT DESIGN

4.1 INTRODUCTION

In this chapter we discuss the characteristics and the controller design strategy only for longitudinal/Pitch plane dynamics of a ballistic missile system, similar approach may be used for lateral/Yaw dynamics. Sliding mode control strategy is employed in this research because of its inherent insensitivity and robustness to plant uncertainties and external disturbances. The stability of the system is ensured in the design procedure via Lyapunov direct method. This chapter also discusses the sliding mode practical implementation issues and its remedies.

4.2 SLIDING MODE CONTROL

Here we briefly outline SMC design procedure that essentially goes through two stages:

- First stage is to judiciously select the sliding manifold (sliding surface) that exhibits desired performance in the system state space.
- In second stage state feedback control law is designed which ensures the attractiveness of this sliding manifold as depicted in Fig. 4.1 from any given initial conditions for the states of the system. The control law usually consists of two additive terms [2], [26].

$$\mathbf{u} = \mathbf{u}_{eq} + \mathbf{u}_{in} \quad 4.1$$

In case of the full information of the plant and the external disturbances, the term u_{eq} , called equivalent control, which can be determined to provide exact, $S = 0$. In the uncertain case it is substituted by its estimate, \hat{u}_{eq} of any portion of u_{eq} which can be estimated or calculated.

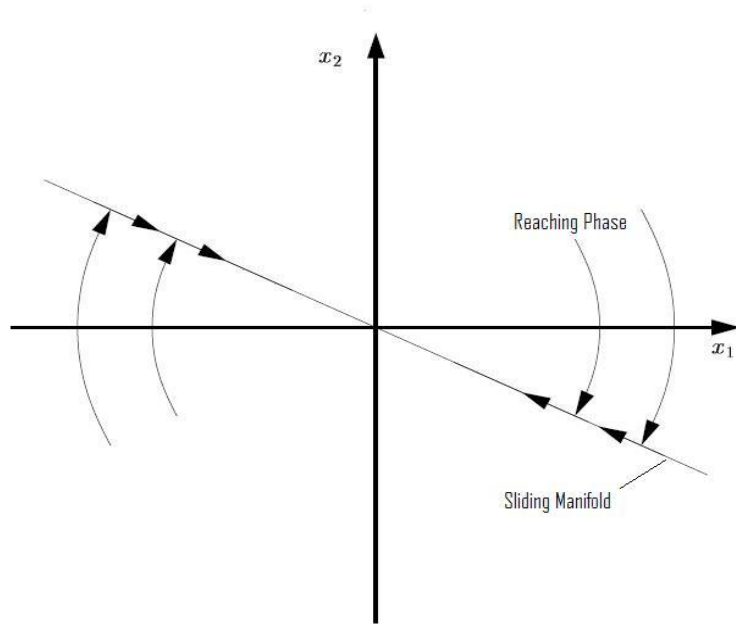


Fig. 4.1 General SMC Graphical Illustration

Rest of the uncertainty is captured by other part, u_{un} , called uncertain control which is additive and complementary to \hat{u}_{eq} and can capture even total uncertain u_{eq} i.e. $\hat{u}_{eq} = 0$. If constant rate reaching law is employed then the sliding control becomes [21].

$$u_{un} = \delta = \dot{S} = -K_1 \text{sgn}(S) \quad 4.2$$

Missile autopilots are usually designed to track acceleration commanded by a guidance law on the basis of data sensed and estimated by a navigation system, where a widely accepted approach is to estimate relative position, velocity and acceleration via extended Kalman filtering technique [2]. A general structure for SMC based missile autopilot is shown in Fig.4.2 [2].

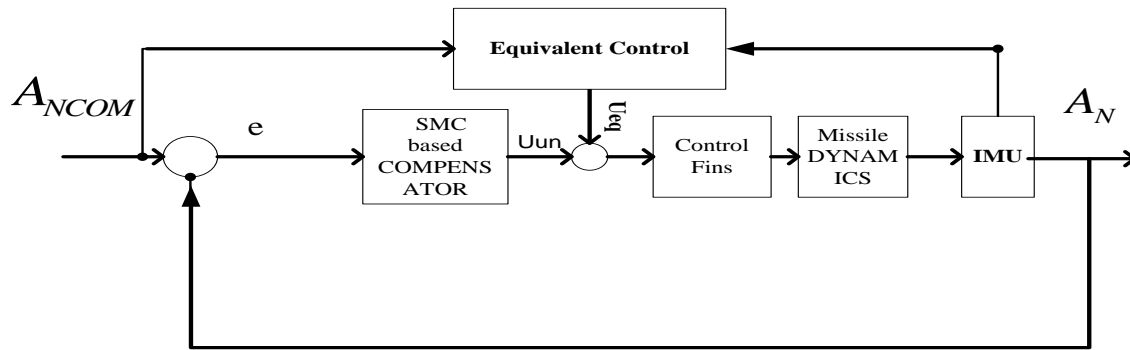


Fig. 4.2 General SMC based Missile Autopilot Structure

where,

A_{NCOM}	Commanded Normal Acceleration
A_N	Achieved Normal Acceleration
u_{un}	Uncertain Control
u_{eq}	Equivalent Control
e	Acceleration Error

4.3 PROPOSED CONTROL STRATEGY

Since cross couplings have very less effect on the pitch channel provided that if the roll and yaw rates are not high, so far designing the autopilot for a ballistic missile which posses these characteristic we assume the pitch channel as a separate channel whose motion is uncoupled with other two channels.

In this section we design a new SMC based autopilot system for pitch channel only and then apply all the corrections, adaptations and gain tuning if necessary to achieve stability, robustness and performance. Similar approach may be employed for other channels as well. Here we propose the concept of multiple sliding surfaces “ S_1, S_2 ” based on normal position and velocity deviations when a trajectory following guidance is employed as

$$S_1 = G_1 \varepsilon_z \quad 4.5$$

$$S_2 = G_2 \varepsilon_{V_z} \quad 4.6$$

Where,

G_1, G_2 , Strictly Positive, Gains.

ε_z Normal Position Guidance, Deviation.

ε_{V_z} Velocity Normal Component, Deviation.

The advantage of selecting these surfaces is that by choosing these surfaces we can make control independent of the system parameters resulting in increased robustness to system parametric variations. For our case plant is assumed to be totally uncertain, hence $u_{eq} = 0$ in this case $u = u_{im}$ will be used to steer the system towards the sliding mode “ $S_1 = 0$ and, $S_2 = 0$ ” [2], [26], thus the basic idea is the enforcement of two dimensional sliding mode in the intersection of two discontinuity surfaces, as depicted in Fig. 4.3, such that the system always reach and track the intersection of the surfaces “ $S_1 = 0$ and, $S_2 = 0$ ”, and thus minimizing the positional and velocity guidance errors which in turn minimize the range error.

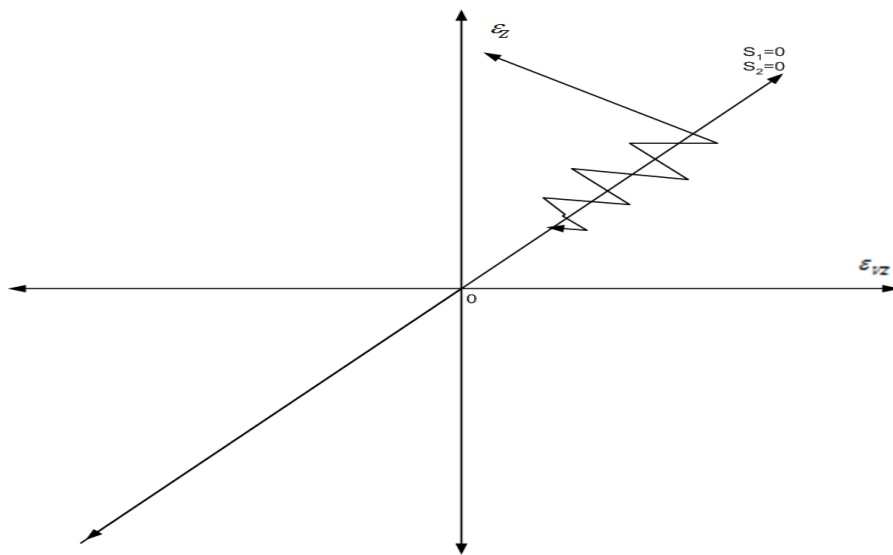


Fig. 4.3 Convergence of States to the Intersection of Sliding Surfaces

The overall control (Elevator deflection angle δ in our case) to ensure the system stability (robustness) is based on constant rate reaching laws [21] defined on multiple surfaces S_1 and S_2 as,

$$\delta = \dot{S}_1 + \dot{S}_2 \quad 4.7$$

$$\delta = -K_1 \text{sgn}(S_1) - K_2 \text{sgn}(S_2) \quad 4.8$$

The above control law depicts that when both $S_1=0$ and $S_2=0$, i-e Positional and Velocity guidance deviations become zero; control (elevator fin deflection) would also equals zero.

4.4 SYSTEM STABILITY ANALYSIS

To ensure stability of the system is an important factor while designing and analyzing a flight control system. Lyapunov direct method plays an important role to analyze the stability of nonlinear control system. One of the advantages of sliding mode control is that one can ensure the system stability while designing the control law using Lyapunav direct method. In our case vehicle is assumed to be aerodynamically (statically) stable because it was ensured while air frame design that its center of pressure always lies behind the center of gravity through out the flight regime (or simply M_α is always negative). The nonlinear system stability after controller implementation is ensured by Lyapunov function defined by

$$V(S_1, S_2) = \frac{1}{2} (S_1^2 + S_2^2) \quad 4.9$$

And its derivative is

$$\dot{V} = S_1 \dot{S}_1 + S_2 \dot{S}_2 \quad 4.10$$

Where \dot{S}_1 and \dot{S}_2 are defined by constant rate reaching laws as given in control law and thus

$$\dot{V} = -K_1 S_1 \text{sgn}(S_1) - K_2 S_2 \text{sgn}(S_2) \quad 4.11$$

This will always result in

$$\dot{V} = -(K_1|S_1| + K_2|S_2|) \quad 4.12$$

Where K_1 and K_2 are positive gains and thus, \dot{V} will remain negative definite hence system asymptotic stability is ensured.

4.5 TUNING PROCEDURE

The basic tuning is tradeoff, between desired settling time and the agility of the command profiles to follow without loss of stability and maintain position guidance error, velocity guidance error, acceleration and pitch rates within limits. Also to get desired performance any rate reaching law may be used. Similar design approach may be used for Yaw autopilot. The parameters, K_1, K_2, G_1, G_2 , (See Appendix A) were calculated by successive simulations to achieve optimum control performance. Nonlinear SixDOF simulator has the provision to select different gains at different time instants. An excessive increase in K_1, K_2, G_1, G_2 results in fast but more oscillatory response and high steady state error, therefore, gain setting was a compromise between speed of response and the steady state error.

4.6 SMC IMPLEMENTATION

Switching control law is not energy saving and in case when control is fins deflection angle, they can't move instantly. Imperfections in the switching are the major limitation to Sliding mode control to become a universal control. Switched control signal may excite high frequency dynamics of the system neglected in the course of modeling such as un-modeled structural modes, time delays and so on. This causes fast, finite amplitude oscillations in the vicinity of sliding surface known as “chattering” as depicted in Fig.4.4 which results in loud noise, high wear of moving mechanical parts and thus should be definitely eliminated. Different schemes have been proposed in the research literature to eliminate the chattering [22]-[26].

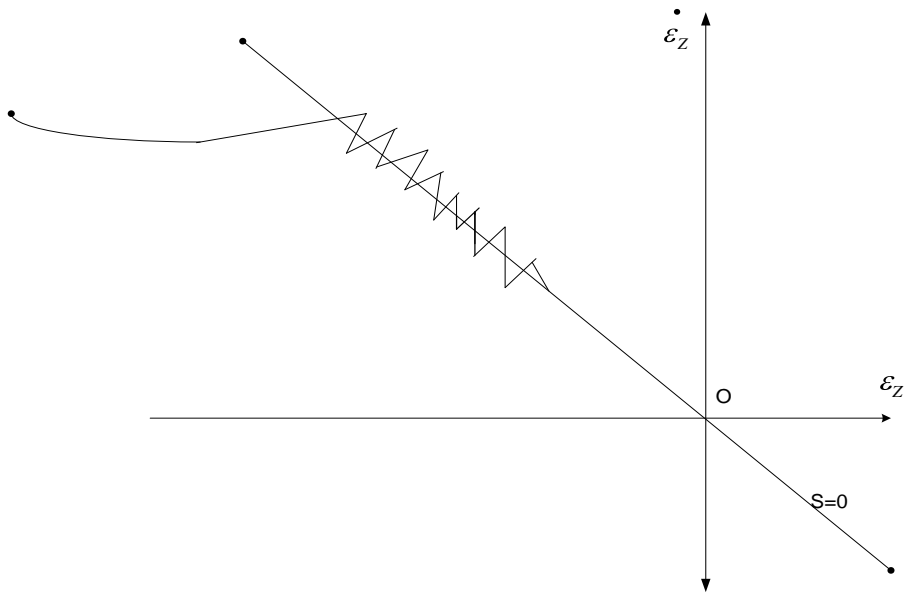


Fig. 4.4 Chattering Phenomenon

The most commonly cited approach to reduce the effects of chattering has been the so called piecewise linear or smooth approximation of the switching element in a boundary layer in the vicinity of the sliding surface. This can be achieved by smoothing out the control discontinuity by replacing signum function with saturation function as depicted in Fig.4.5

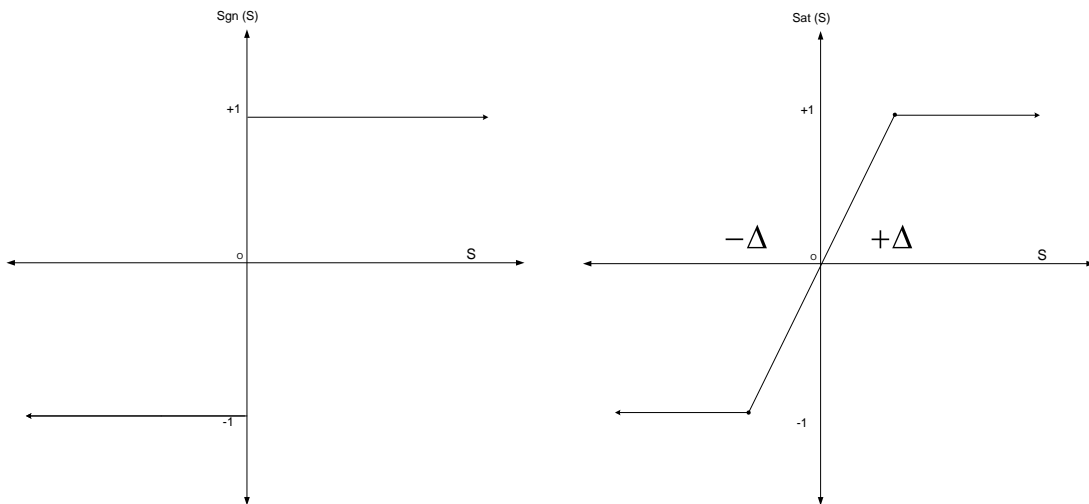


Fig. 4.5 Signum and Saturation function

Mathematically,

$$Sgn(S) = \begin{cases} 1 & S > 0 \\ 0 & S = 0 \\ -1 & S < 0 \end{cases} \quad \& \quad Sat(S) = \begin{cases} 1 & S > \Delta \\ S/\Delta & |S| \leq \Delta \\ -1 & S < -\Delta \end{cases} \quad 4.13$$

Selection of the boundary layer of saturation function is basically a compromise between the system robustness and chattering suppression, In this design we have selected the boundary layer length “ $\Delta = \pm 1$ ”. The resulting control with chattering suppression is

$$\delta = -K_1 sat(S_1) - K_2 sat(S_2) \quad 4.14$$

This design makes the system completely independent of system parameters and also it provides various gains tuning options i-e, K_1, K_2 and also S_1, S_2 depends on G_1, G_2 , hence it results in improved system robustness to system parametric variations as compared to already presented designs.

4.7 SUMMARY

In this chapter a robust autopilot structure for longitudinal dynamics of a ballistic missile was developed using sliding mode control technique. This design makes the system completely independent of system parameters and also it provides various gain tuning options hence it results in improved system robustness as compared to already presented designs. Stability of the system was ensured in the design procedure via Lyapunov direct method. SMC practical implementation issues and its remedies were also discussed. Similar approach may be used for lateral dynamics/Yaw autopilots.

RESULTS AND ANALYSIS

5.1 INTRODUCTION

In the previous chapter we developed and proposed a robust autopilot structure for pitch motion of a ballistic missile system. In this chapter we will show the performance of controller for throughout the flight, which ensures that the controller is meeting the design criterion. We will discuss the performance of controller for complete flight trajectory using SixDOF/nonlinear simulations in the presence of environmental disturbances, like thrust misalignment and drag variation etc. The linear dynamics developed in chapter 3 will be validated and compared with actual SixDOF Nonlinear dynamics. Linear system results will also be discussed for acceleration autopilot. The Nonlinear/SixDOF is software developed in FORTRAN and C/C++ which contains nonlinear dynamics of the missile system i.e. nonlinear equations of forces and moments. It provides us with a simulated environment of Guidance, Navigation and Control files, in which we may also introduce the environmental disturbances such as thrust misalignment and drag variation and parametric variations etc. as a result of this simulator designed controller may be easily embedded on the practical system using digital signal processors. In short Nonlinear SixDOF simulator provides a development platform for building and testing new control algorithms for aerial vehicles. We will also analyze the robustness of the controller by varying the disturbances and parameters of plant using Nonlinear SixDOF simulator.

5.2 DYNAMICS VALIDATION

In this section, the system dynamics developed in chapter 3 would be verified using SIXDOF/Nonlinear Simulator. For the force and moment coefficients given in Appendix B, and the control input “ δ ” shown in Fig. 5.1 was given to Nonlinear/SixDOF simulator and the linear system dynamics developed in chapter 3 for system state variables α (angle of attack) and q pitch rate, comparison of outputs from both the Nonlinear simulator and linear dynamics developed in chapter 3 are shown in following figures (Fig 5.2 and Fig. 5.3), where Linear dynamics results and the Nonlinear Simulator results are compared. From these graphs it may be

concluded that the linear dynamics developed for a tail controlled ballistic missile system in chapter 3 is comparable with the actual nonlinear system simulator dynamics.

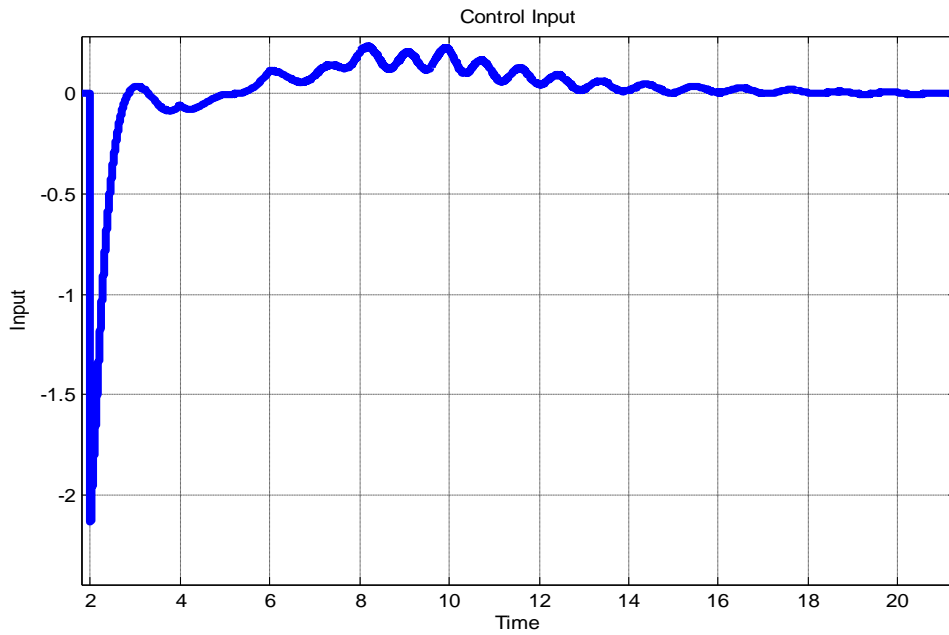


Fig. 5.1 Control Input “ δ ” Given to the System

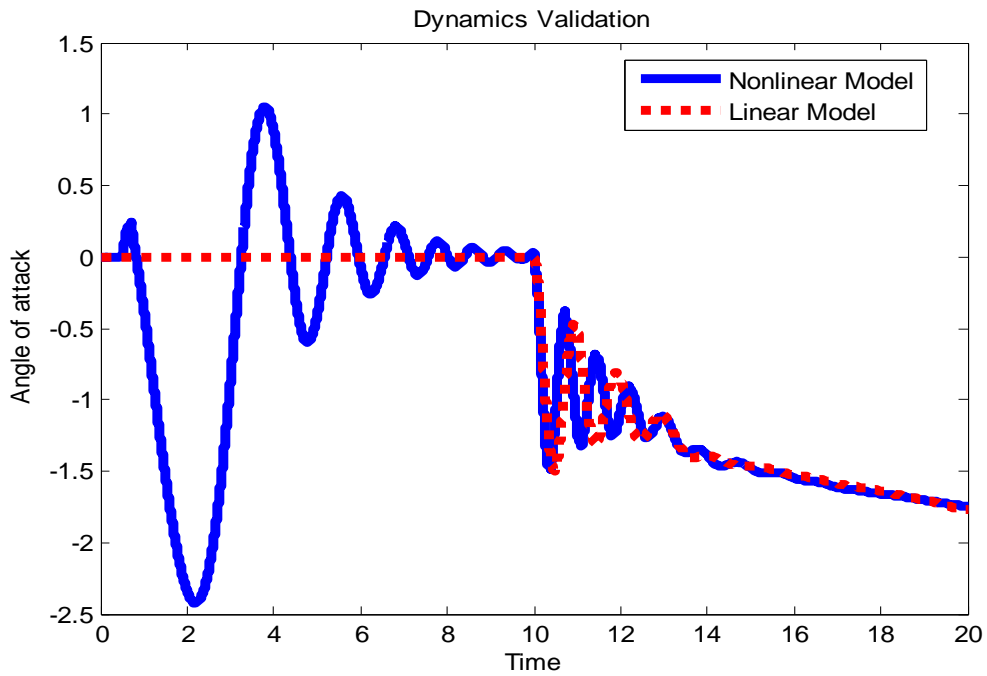


Fig.5.2 Angle of Attack

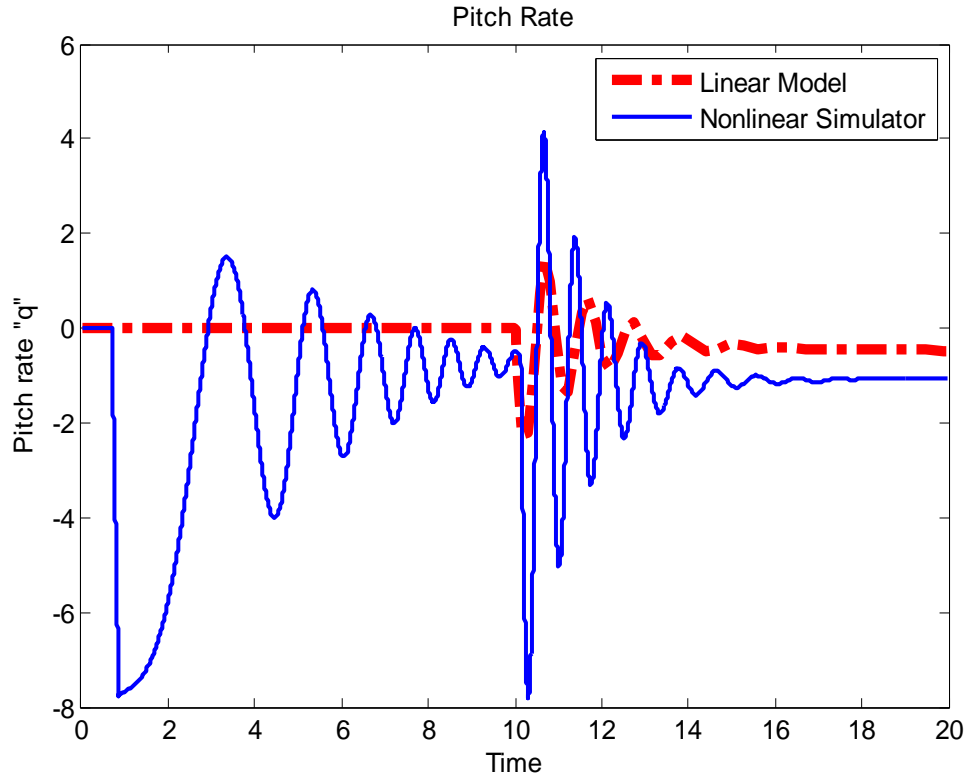


Fig. 5.3 Pitch Angle Rates

5.3 LINEAR SYSTEM SIMULATION

Before discussing the simulations for actual nonlinear system using SixDof/ Nonlinear simulator here we briefly discuss the linear system results using conventional SMC approach defined by

$$S = G \times \varepsilon_A \quad 4.5$$

Where G , is a positive gain and ε_A is acceleration error. The Sliding control with chattering suppression is given as

$$\delta = -K \times \text{sgn}(S) \quad 4.14$$

Where, K is strictly positive gain. Simulation was carried using Matlab/Simulink for representative numerical values of various parameters [19] given in below table for an acceleration step input of 45 degree; the system response is shown in Fig. 5.4.

Table 5.1 Matlab Simulation parameters

M_α	$-248rad / sec^2$
M_δ	$-662rad / sec$
V	$382m / sec$
Z_α	$-1271 / sec^2$
Z_δ	$-340m / sec^2$

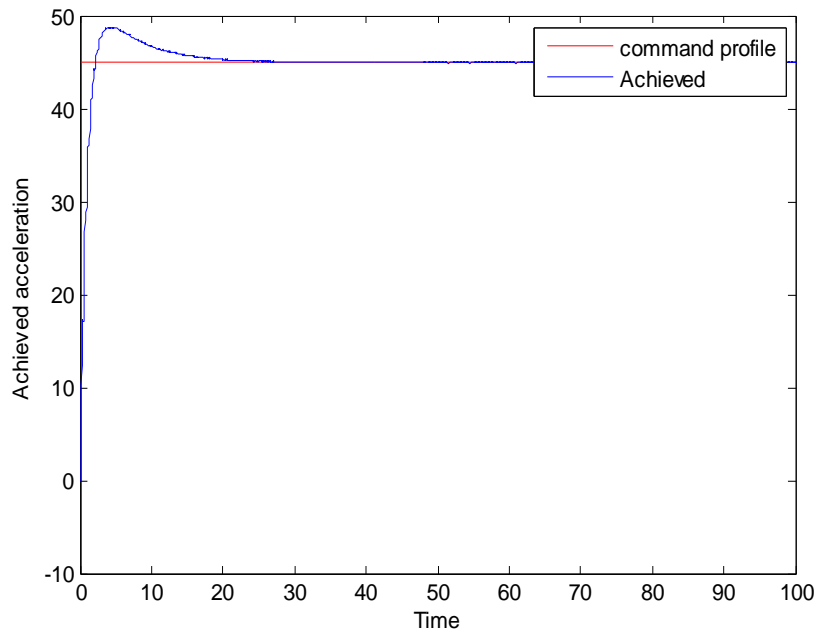


Fig. 5.4 Normal Acceleration Tracking

The acceleration autopilot suffers from inverse step response initially due to the presence of right half plane zero in the system transfer function as depicted in Fig. 5.5

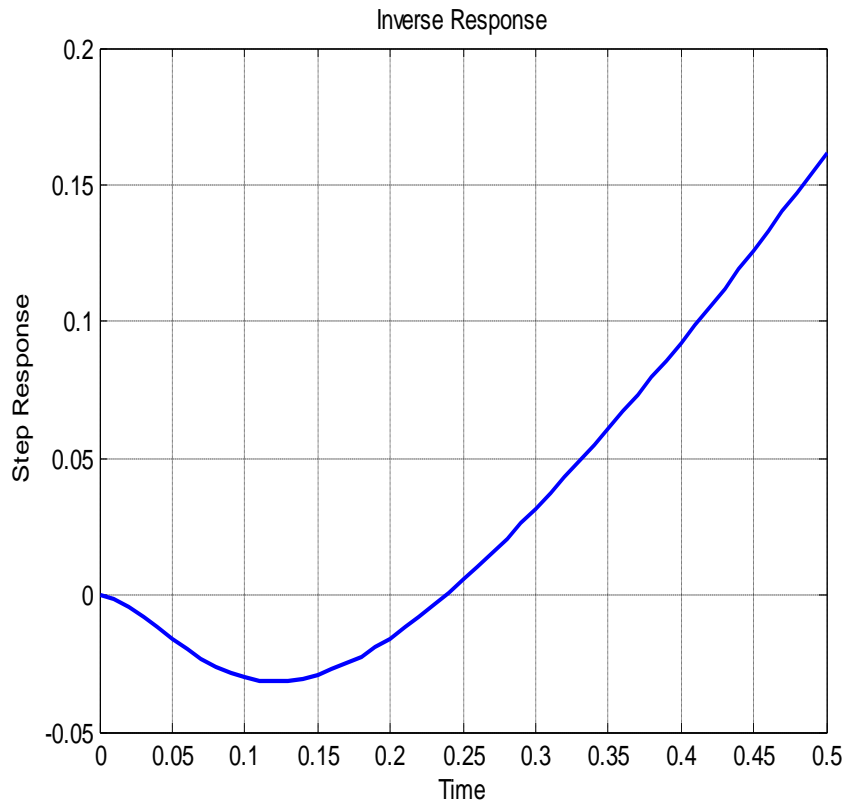


Fig. 5.5 Inital Inverse Step Response

Next the system response using proposed control structure will be presented which completely replaces acceleration autopilot.

5.4 SIMULATIONS USING NONLINEAR/SIXDOF SIMULATOR

Since the proposed control structure is based on the minimization of nonlinear guidance errors calculated in Nonlinear /SixDOF simulator from the range versus trajectory graph, It is not possible to simulate this approach in Matlab/Simulink using Linear or Nonlinear system dynamics because it requires advanced trajectory Guidance, Navigation and Control built-in features of a Nonlinear/SixDOF Simulator and trajectory linear model. Therefore proposed control structure was directly applied to the Nonlinear/SixDOF simulator and optimum control was designed, its brief results are discussed here. The idea of control is similar to minimization of the acceleration error in commonly used missile autopilots as discussed in previous section for linear system, in our case we minimize the nonlinear position and velocity guidance errors calculated with respect to trajectory in nonlinear SixDOF simulator.

Simulations were performed for representative numerical values for a tail controlled ballistic missile system for a range of 160 km, for nominal case time varying disturbances like drag variation, thrust misalignment, wind profile and uncertainties in the estimated force and moment control derivatives used to calculate the aerodynamic data obtained through DATCOM software (see Appendix B), while parameters, K_1, K_2, G_1, G_2 , (See Appendix A) were calculated by running successive simulations to achieve optimum control performance (excessive increase in K_1, K_2, G_1, G_2 results in fast but more oscillatory response and high steady state error, so gain setting was a compromise between speed of response and the steady state error) . Simulation results shown in following figures justify the validity of the proposed control structure. Simulations were performed in the Nonlinear SIXDOF simulator, which actually simulates the three dimensional nonlinear motion of the missile so that the designed controller may be easily embedded on the practical system. A number of simulations using proposed control strategy were carried out with the nominal values of below mentioned disturbances and aerodynamic data obtained through DATCOM software, until an optimized performance was obtained. The designed system was then checked for Robustness against variations of disturbances and flight data.

The software had the provision to include the following environmental disturbances

- ISP (Specific Impulse) is the deviation from the normal thrust expressed in percentage of the nominal value.
- Thrust Misalignment is the deviations of the Nozzle's position from the reference zero position.
- Drag variation is defined as the variation in the resistance to airflow from the normal value.

Controller was firstly designed for nominal disturbances and nominal flight data obtained through DATCOM software (see Appendix B) for a flight trajectory of 160 Km Range to get optimum control of various parameters as depicted in following figures (position guidance error, velocity guidance error, pitch rates, elevator command deflection, acceleration command tracking and flight trajectory tracking), the figure of merit (FOM) of each of the parameter is also described below each figure. These plots were obtained from Matlab program using the data obtained through Nonlinear SixDOF simulator.

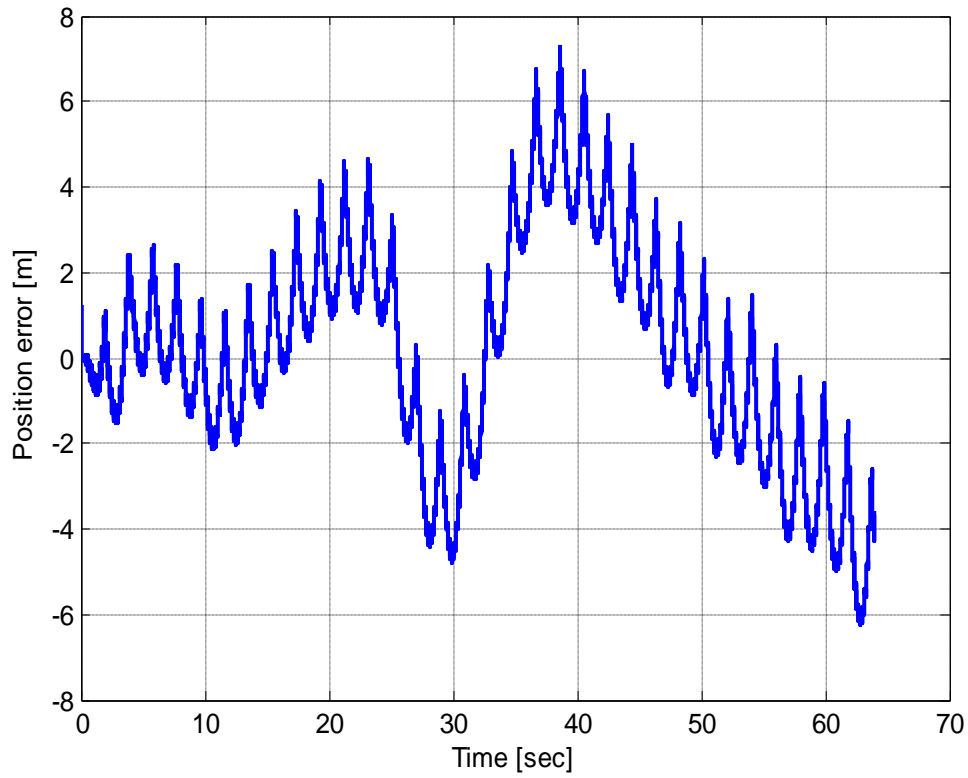


Fig. 5.6 Positional Guidance Error

Fig. 5.6 depicts that the system was designed to maintain the positional guidance error remain within 10 meters of the desired nominal trajectory guidance. Allowable error is 300 m.

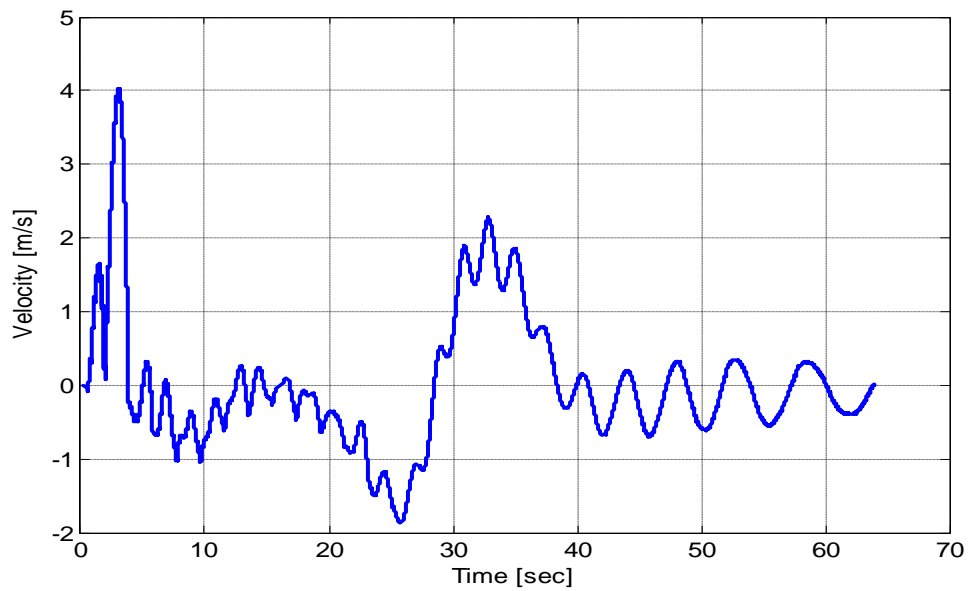


Fig. 5.7 Velocity Guidance Error

Fig. 5.7 depicts that the system was designed to maintain the velocity guidance error remains within 5 meters of desired nominal trajectory guidance. Figure of merit for velocity guidance error is 50 m/sec

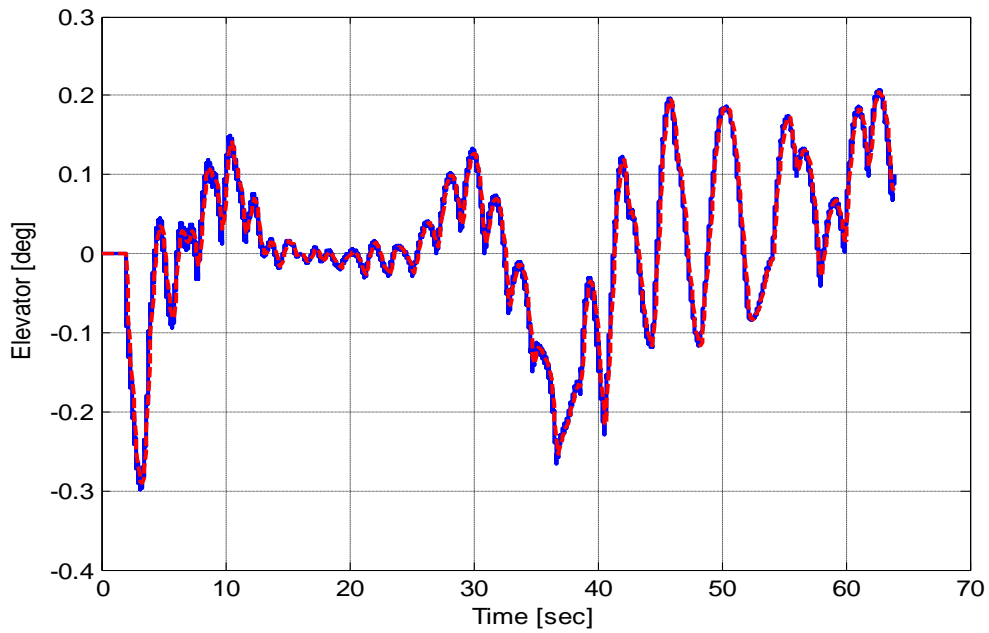


Fig. 5.8 Elevator Fin Deflection

In Fig. 5.8 Elevator, the control command generated does not saturate at 4-degree deflection limit and is also within the actuator limits of 4-degree.

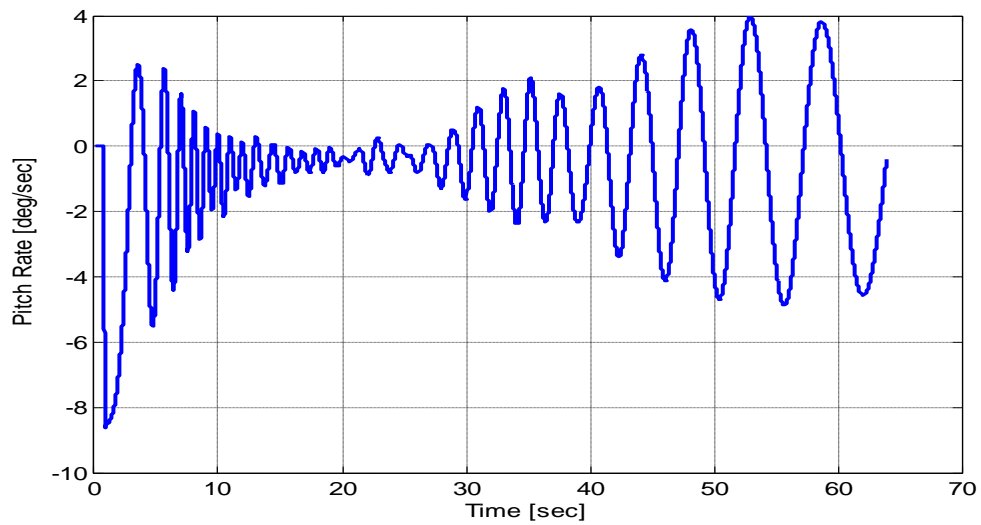


Fig. 5.9 Body Pitch Rates

Fig. 5.9 Body pitch rates are within gyros saturation rate limit of 10 degree/second.

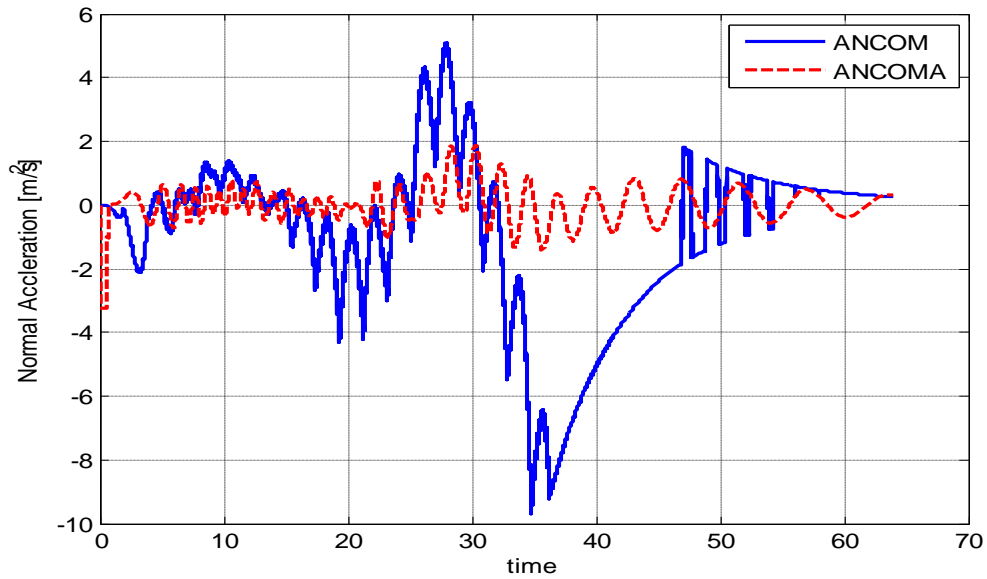


Fig. 5.10 Acceleration Command Tracking

Fig. 5.10 depicts that acceleration command is also automatically tracked and remain within missile acceleration capability of $40 m/sec^2$. Where ANCOM is commanded normal acceleration and ANCOMA is achieved normal acceleration.

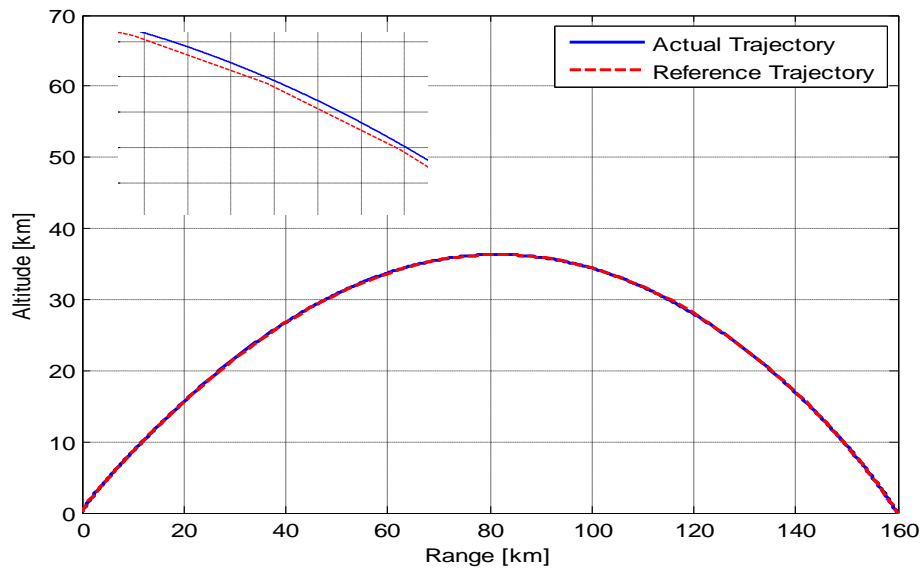


Fig. 5.11 Flight Trajectory for Nominal Disturbances

Fig 5.11 depicts trajectory tracking and minimization of range error within 100 meter of the impact point. Allowable range error is 300m.

5.5 SYSTEM ROBUSTNESS ANALYSIS

The overall closed loop control system was also checked for robustness against parameter variations (parametric uncertainties) and time varying disturbances (disturbance uncertainties). The results of worst possible cases are discussed here

Case 1:

The disturbances in Table 5.1 are the worst case disturbances for increasing range because all the disturbances force the missile to go more ahead than desired. It is seen from the figures (position guidance error, velocity guidance error, pitch rates, elevator command deflection, acceleration command tracking and flight trajectory tracking) below that controller performed very well in the presence of these errors and made the vehicle to follow the desired trajectory with a range error of +70 meters only whereas the maximum allowable error in the range is of 300 meters.

Table 5.2 Applied Disturbances and parametric variations

ISP Deviation	2%		
Thrust Misalignment	0.7 mili radian		
Wind	7 -124 meter/second (In missile direction)		
Drag Variation	-4%		
Parametric variations	M_δ	+10%	Z_α +10%
	M_α	+10%	Z_δ +10%

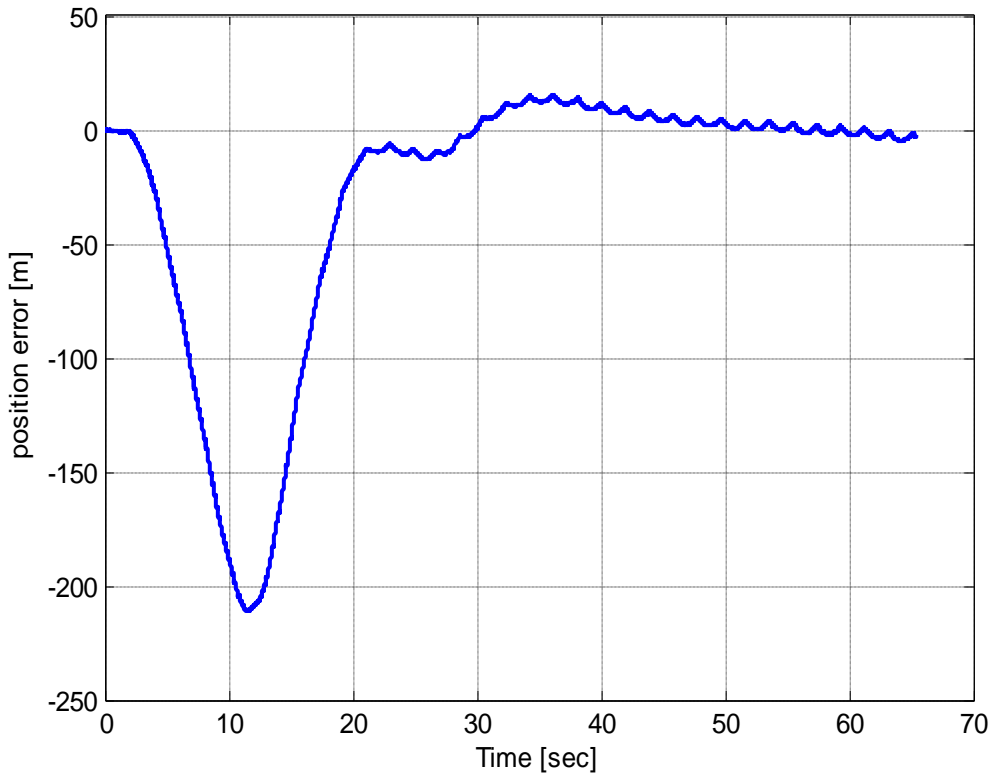


Fig. 5.12 Positional Guidance Error

Fig. 5.12 depicts that the system was designed to maintain the positional guidance error remain within 230 of the desired trajectory guidance. Allowable error is 300 m.

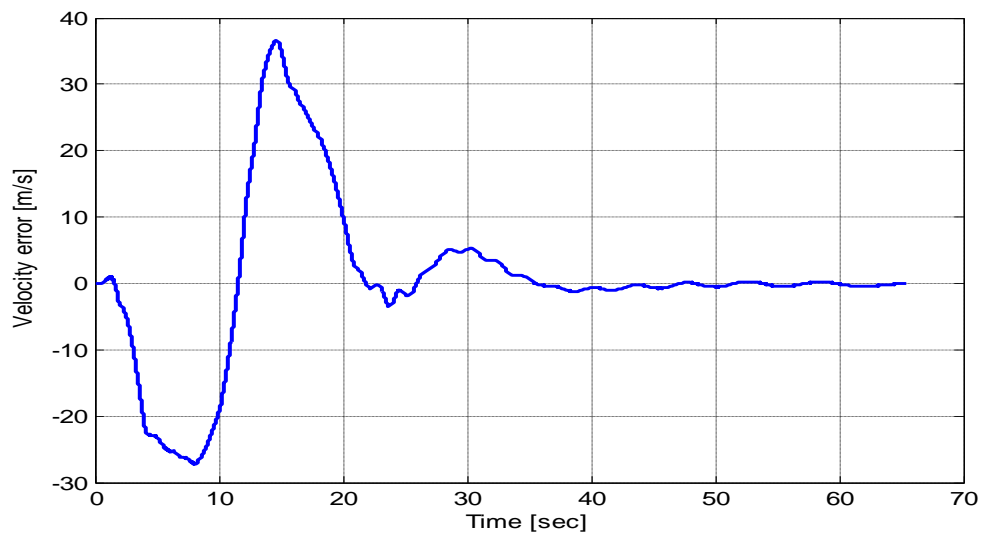


Fig. 5.13 Velocity Guidance Error

Fig. 5.13 depicts that the system was designed to maintain the velocity guidance error remains within 40 meters; Figure of merit for velocity guidance error is 50 m/sec.

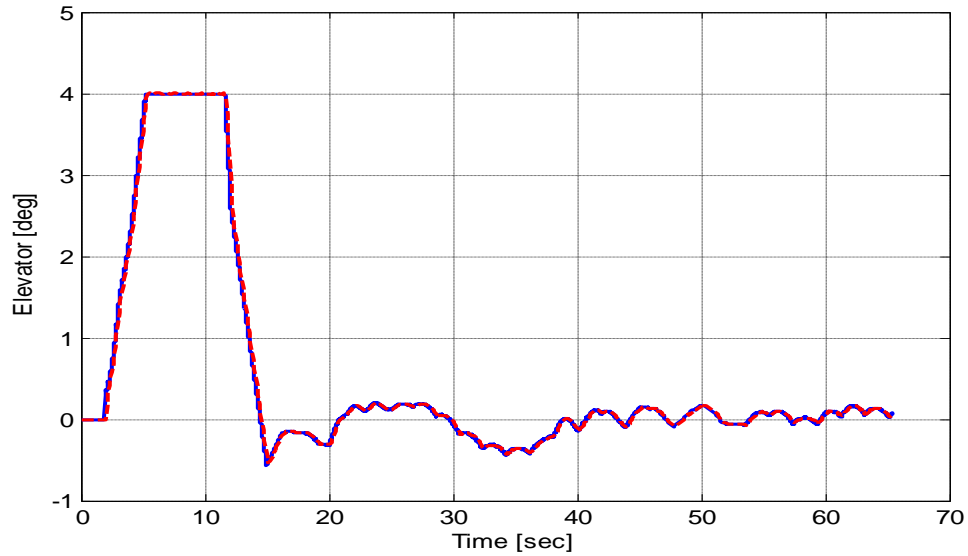


Fig. 5.14 Elevator Fin Deflection

In Fig. 5.14 Elevator, the control command generated saturates at 4 degree deflection limit, and is also within the actuator limits of 4-degree.

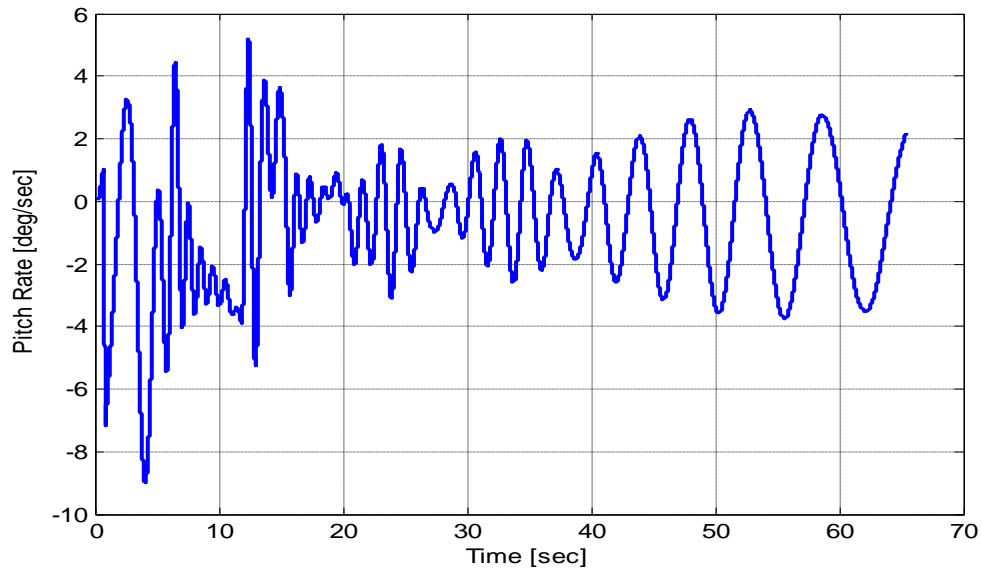


Fig. 5.15 Body Pitch Rates

In Fig. 5.15 Body pitch rates are within gyros saturation rate of 10 degree/second.

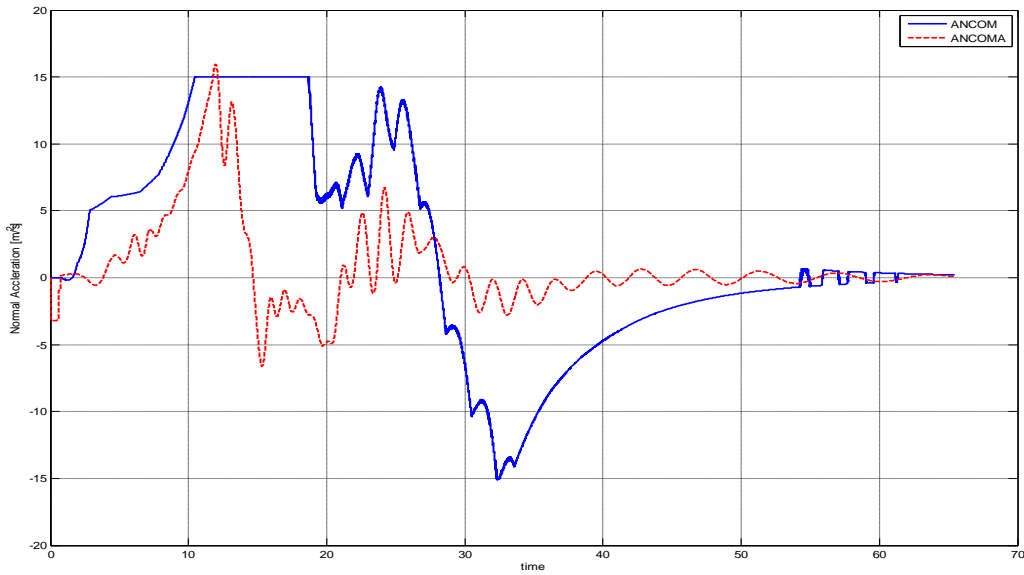


Fig. 5.16 Acceleration Command Tracking

Fig. 5.16 depicts that acceleration command is also automatically tracked and remain within missile acceleration capability of $40 m/sec^2$. Where ANCOM is commanded normal acceleration and ANCOMA is achieved normal acceleration.

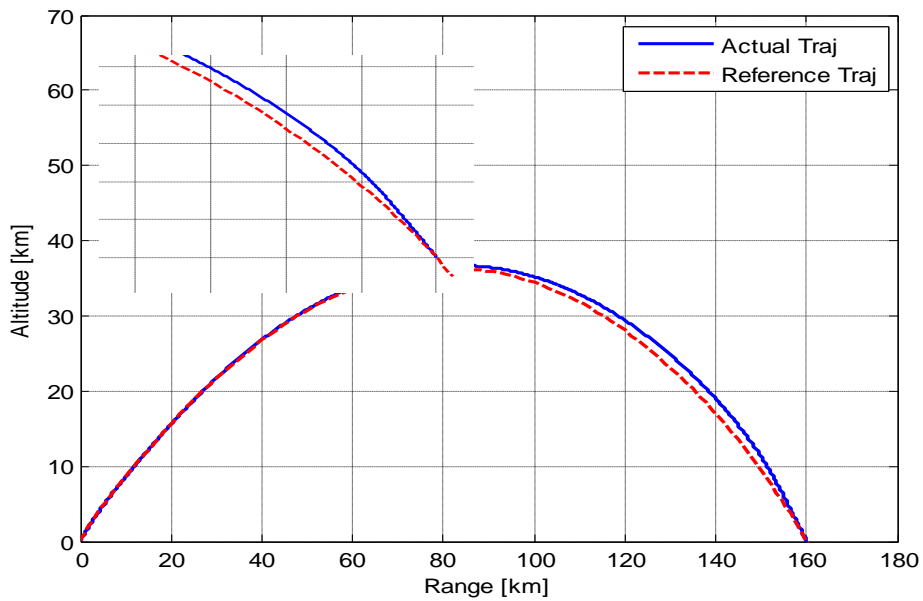


Fig. 5.17 Flight Trajectory with Increasing Range Disturbances

Fig 5.17 depicts Trajectory tracking and minimization of range error within 100 meter of the impact point, whereas the maximum allowable error in the range is of 300 meters.

Case 2:

The disturbances in Table 5.2 are the worst case disturbances for decreasing range because all these disturbances force the missile to remain behind the desired trajectory. It is seen from the figures (position guidance error, velocity guidance error, pitch rates, elevator command deflection, acceleration command tracking and flight trajectory tracking) below that controller performed very well in the presence of these errors and made the vehicle to follow the desired trajectory with a range error of -50 meters only whereas the maximum allowable error in the range is of 300 meters.

Table 5.3 Applied Disturbances and Parametric Variations

ISP Deviation	0%			
Thrust Misalignment	0.7 mili radian			
Wind	7 -124 meter/second (opposite direction)			
Drag Variation	+4%			
Parametric variations	M_{δ}	-10%	Z_{α}	-10%
	M_{α}	-10%	Z_{δ}	-10%

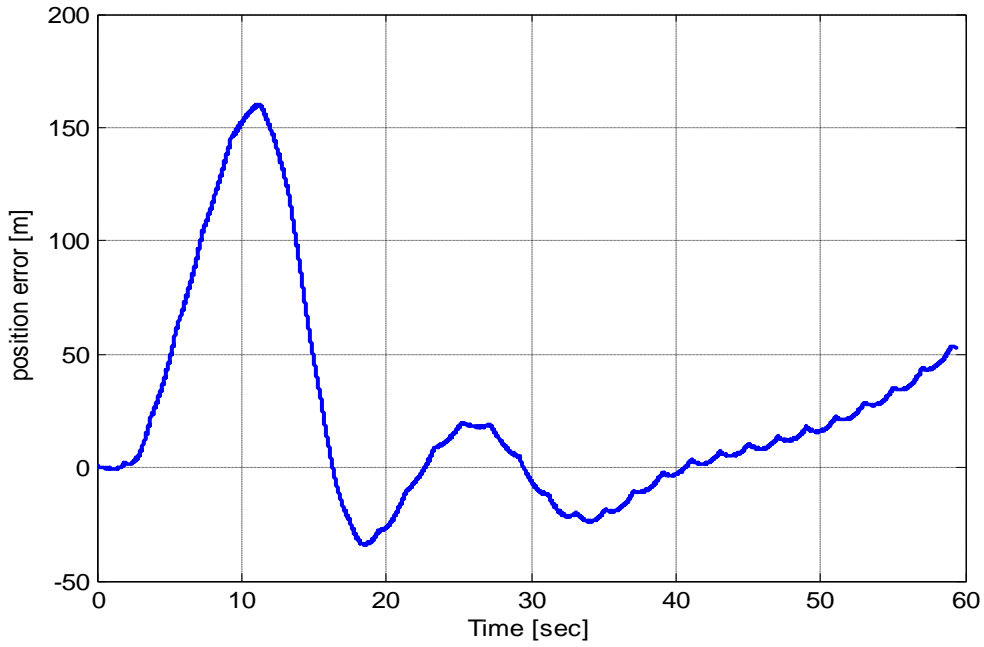


Fig. 5.18 Positional Guidance Error

Fig 5.18 depicts that the system was designed to maintain the positional guidance error remain within 200 meters of the trajectory guidance. Allowable error is 300 m.

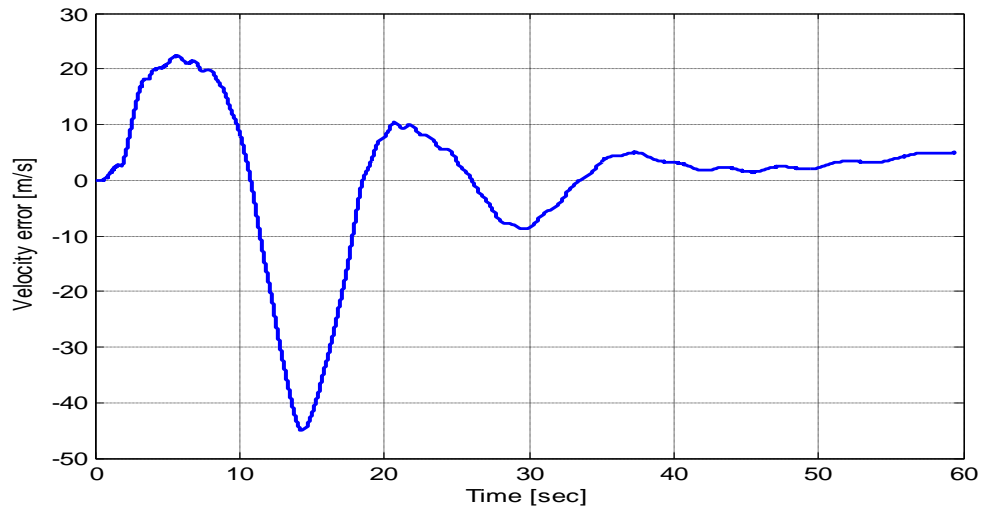


Fig. 5.19 Velocity Guidance Error

Fig. 5.19 depicts that the system was designed to maintain the velocity guidance error remains within 50 meters of the desired trajectory guidance. Figure of merit for velocity guidance error is 50 m/sec.

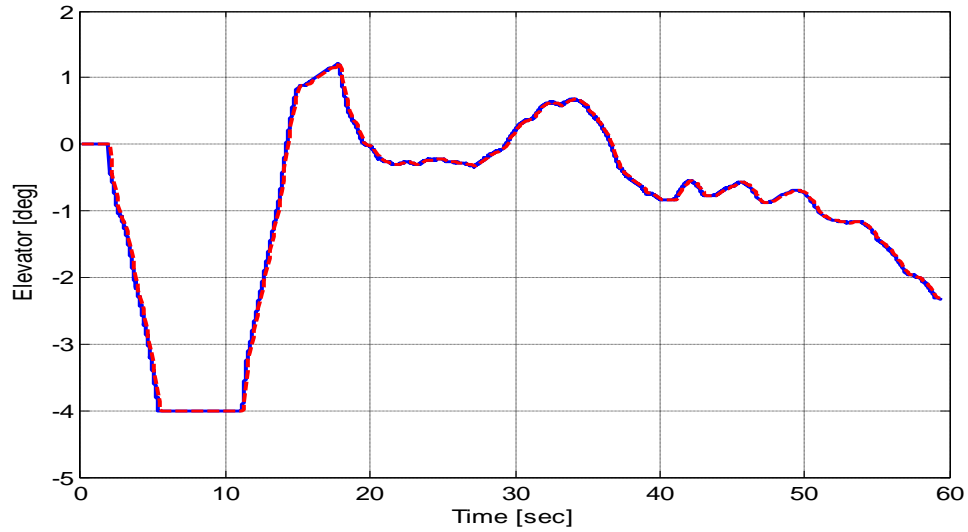


Fig. 5.20 Elevator Fin Deflection

In Fig. 5.20 Elevator, the command generated saturate at -4 degree deflection limit and is also within the actuator limits of 4-degree.

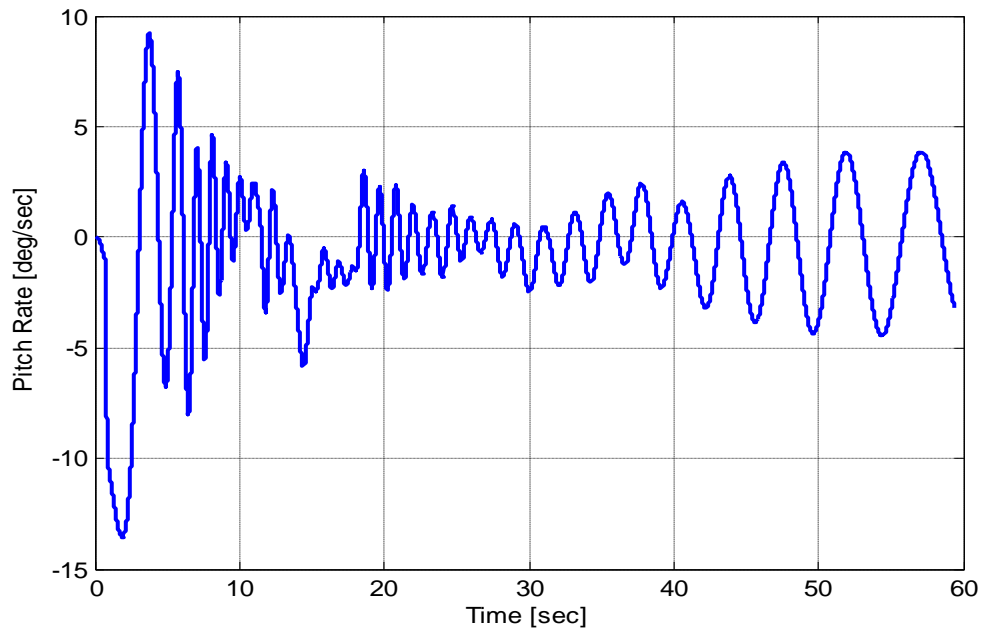


Fig. 5.21 Body Pitch Rates

In Fig. 5.21 Body pitch rates are within gyros saturation rate of 10 degree/second.

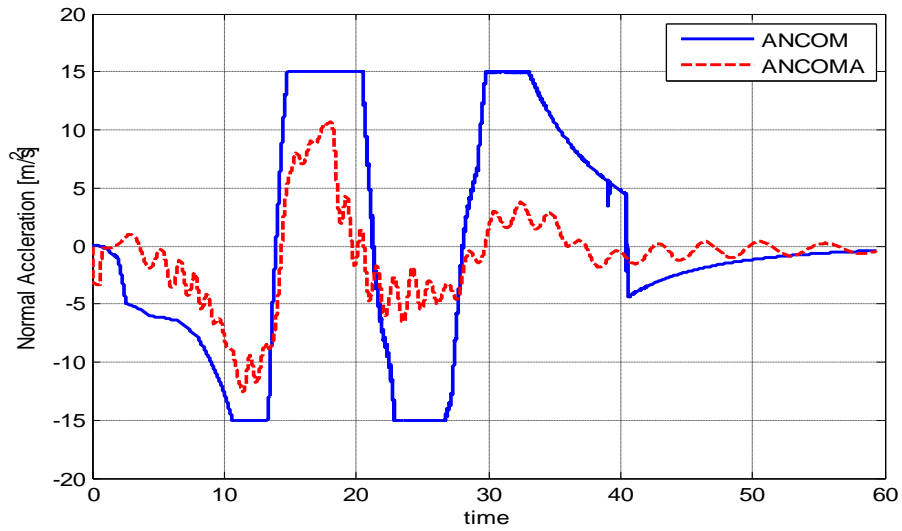


Fig. 5.22 Acceleration Command Tracking

Fig. 5.22 depicts that acceleration command is also automatically tracked and remain within missile acceleration capability of 40 m/sec^2 . Where ANCOM is commanded normal acceleration and ANCOMA is achieved normal acceleration.

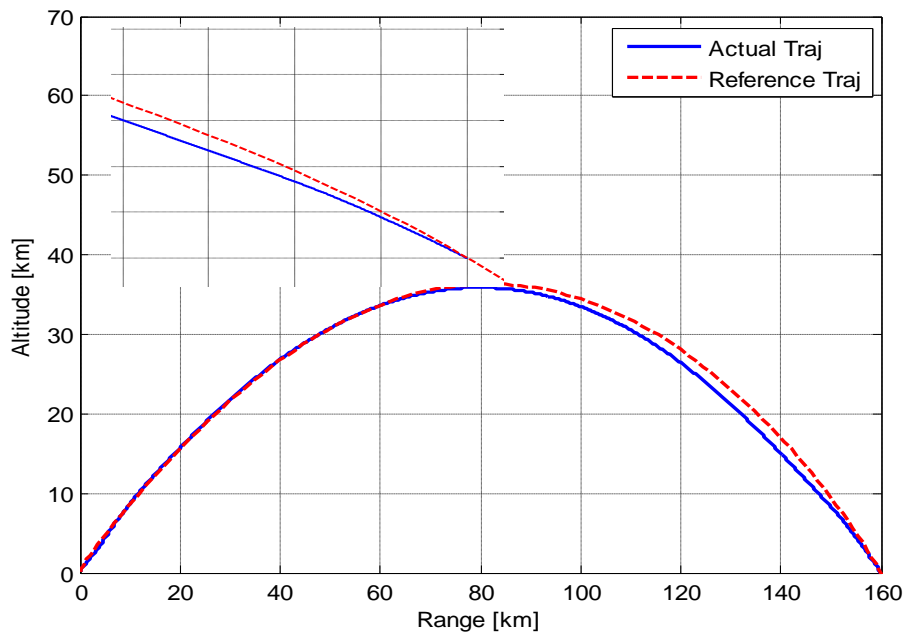


Fig. 5.23 Flight Trajectory with Decreasing Range Disturbance

Fig. 5.23 depicts Trajectory tracking and minimization of range error within 100 meter of the impact point (160 Km). Allowable error is 300 m.

Comparison of results for nominal & worst case increasing and decreasing range disturbances and plant parametric variations are shown in following Table 5.3, which depicts that the designed controller is robust to disturbances and plant uncertainties over a wide range of flight conditions due to changing mach altitude fluctuations. For nominal values of disturbances and plant parameters the system was designed to give only 10 meter range error. It also shows that when system was checked for its robustness to worst cases of increasing and decreasing range disturbances it performed very well giving the range error within 100 meters only whereas the maximum allowable error in the range is of 300 meters.

Table 5.4 Comparison of Results

Case #	Disturbances Applied					Parametric variations	Results
	ISP	Thrust Misalignment mili radian	Wind (m/sec)	Canting	Drag Variation	Force & Moments slopes	Range Error (m)
0	0%	0	Nominal 7 m/sec	0	0	Nominal	10.42
1	0% Drag	7	7-124 (Heading wind)	0	+4%	+10%	-50.5
2	+2% Drag	7	7-124 (Trailing wind)	0.1	-4%	-10%	+70.696

5.6 SUMMARY

In this chapter we analyzed the performance of the proposed control using Nonlinear/SixDof simulator. Simulation results show that the proposed algorithm is able to give good performance regardless of the uncertainties and time varying disturbances. The overall closed loop control system was tested for robustness against parameter variations using nonlinear/SixDOF simulation and is found to exhibit the performance comparable to the one with nominal parameters. Linear system dynamics approximation was also validated on SixDOF Simulator dynamics. Linear system results were also discussed for acceleration autopilot.

CONCLUSION AND FUTURE WORK

6.1 CONCLUSION

In this thesis the design of autopilot for an aerodynamic vehicle was considered for implementing the steering commands obtained from the guidance loop and to ensure a stable flight under the presence of environmental disturbances. In this thesis nonlinear dynamics of a ballistic missile system was presented. The second order linear approximation of the dynamics of the missile was also presented. Linear system dynamics approximation was also validated on SixDOF Simulator dynamics. The dynamics of the system was considered only in the pitch channel and a robust autopilot structure for longitudinal dynamics of a ballistic missile was developed using multiple surface sliding mode control technique due to its inherent insensitivity and robustness properties to plant uncertainties and external disturbances. This design makes the system completely independent of system parameters and, completely replaces conventional acceleration autopilot, giving various gains tuning options and resulting in improved system robustness as compared to already presented designs. It also provides a research platform to apply other robust control techniques and hence provides design flexibility. Stability of the system was ensured in the design procedure via Lyapunov direct method. SMC practical implementation issues and its remedies were also discussed. We analyzed the performance of the proposed control using Nonlinear/SixDof simulator. Simulation results show that the proposed algorithm is able to give good performance regardless of the uncertainties and time varying disturbances. The overall closed loop control system was also tested for robustness against parameter variations using nonlinear/SixDOF simulations, and is found to exhibit the performance comparable to the one with nominal parameters. Similar approach may be used for lateral dynamics/Yaw autopilots.

6.2 BENEFITS

This research results in following advantages.

- Completely replaces Acceleration Autopilot.
- Increased Robustness to time varying disturbance and parametric variations.

- Simple and flexible Design.
- Open doors for Future Research.
- Similar approach may be used for Yaw Autopilots.

6.3 FUTURE WORK RECOMMENDATION

Since a missile system is extremely complex and has very quickly changing dynamics and performs in the presence of both measured and unmeasured disturbances, so there are many directions to work. This research indeed provides a research platform for scientists and engineers working in this area to utilize their knowledge of control engineering for future research.

- Since we have used trajectory following guidance in this research other improved guidance schemes may be employed for better performance.
- There are inaccuracies in the measurement of parameters of the system. Any other different robust technique such as H_∞ can be considered to minimize the guidance errors.
- Proportional –Integral Sliding mode control may be used for robust attitude tracking of a missile system.
- The design of adaptive controller based upon adaptive techniques like self-tuning regulators etc may be considered for the improvement of the performance.
- Similar design approach may be employed for robust control of underwater vehicles and other space vehicles.

AUTOPILOT GAINS

The following table depicts the values of various gain parameters used in the autopilot design. These gains were calculated on hit and trial basis using successive Nonlinear/SixDOF simulations to achieve optimum control performance. Nonlinear SixDOF simulator has the provision to select different gains at different time instants.

Table A Autopilot Gains for Pitch channel

Time	G_1	G_2	K_1	K_2
0	0.01	0.1	0	0
5	0.01	0.1	0	0
10	0.01	0.1	0.00077	0.00077
15	0.01	0.1	0.0014	0.0014
20	0.01	0.1	0.00105	0.00105
25	0.01	0.1	0.00068	0.00068
30	0.01	0.1	0.00036	0.00036
40	0.01	0.1	0.00025	0.00025
50	0.01	0.1	0.00014	0.00014
60	0.01	0.1	0.000114	0.000114
150	0.01	0.1	6.50E-05	6.50E-05
240	0.01	0.1	5.20E-05	5.20E-05

NUMERICAL PARAMETERS

Following table depicts variations with respect to Mach number of various plant parameters. These were obtained through DATCOM software and were simulated in the SixDOF Simulator, where D1 and D2 are drag, disturbance parameters.

Table B System Parametric Variations

Time	M_δ Sec ⁻²	M_α Sec ⁻²	Z_α rad-Sec ⁻²	Z_δ rad-Sec ⁻²	V m-sec ⁻¹	Drag D1	Drag D2
0	-103.87	-87.66	350.79	109.04	1084	0.46	0.38525
5	-109.08	-94.188	366.92	114.55	1054	0.4013	0.32545
10	-112.17	-98.545	375.39	117.9	1043	0.4002	0.3243
30	-119.51	-105.57	385.62	122.19	1030	0.3967	0.322
50	-125.32	-107.73	383.08	125.71	1025	0.417	0.345
100	-129.19	-106.6	377.45	137.41	1020	0.598	0.48
150	-139.64	-128.99	356.24	145.01	1010	0.58	0.44

REFERENCES

- [1] Paul Zarchan, "Tactical and Strategic Missile Guidance," Third Edition, Volume 176, AIAA, 1997.
- [2] I.A. Shklonikov and Y.B. Shtessel, "Robust Missile Autopilot Design Via Higher Order Sliding Mode Control," in *Proc. AIAA Guidance, Navigation and Control Conference*, AIAA-2000-3968,
- [3] M. Bahrami, B. Ebrahimi and, G.R. Ansarifar, "Sliding Mode Observer and Control Design with Adaptive Parameter Estimation for a Supersonic Flight Vehicle" *International journal of aerospace engineering*, volume 2010.
- [4] E. Devaud, H. Siguerdidjane, S. Font, "Some Control Strategies for a High-Angle-of-Attack Missile Autopilot," PERGAMON, *Control Engineering Practice*, Volume. 8, 2000, pp. 885-892.
- [5] R.A. Nichols, R.T. Reichert, and W.J. Rugh (1993), "Gain Scheduling for H-infinity Controllers: a flight control example," *IEEE Transactions on Control Systems Technology*, Volume.1, No.2, 1993, pp. 69–78.
- [6] Richard A, Hull, Darren Schumacher, Zhihua, "Design and Evaluation of Robust Nonlinear Missile Autopilots from a performance perspective," *Proceedings of American Control conference*, Washington, 1995.
- [7] Michael B. Mcfarland and Christopher N.D. Soura, "Missile Autopilot Design using Dynamic Inversion and Structured Singular Value Synthesis," U.S Air force Armament directorate, USA.
- [8] Abhijit Das, Ranajit Das, Sidhartha Mukhopadhyay, Amit Patra "Robust Nonlinear Design of three Axes Missile Autopilot via Feedback Linearization," [online available].
- [9] H.J. Uang, B.S Chen, "Robust Adaptive Optimal Tracking Design for Uncertain Missile Systems: A Fuzzy Approach," *Journal of Fuzzy Sets and Systems*, Volume 126, pp. 63-87, 2002.
- [10] Parasad Parkhi, Bijnan Bandyopadhyay and Mahendra Jha, "Design of Roll Autopilot for a Tail Controlled Missile Using Sliding Mode Technique," in *Proc. 11th International Workshop on Variable Structure Systems*, 2010.

- [11] M.U. Salamci, M.K. Ozgoren and S.P. Banks, "Sliding Mode Control with Optimal Sliding Surfaces for Missile Autopilot Design," *Journal of Guidance, Control and Dynamics*, Vol. 23, No. 4, 2000.
- [12] J. Moon and Y. Kim , "Design of Missile Guidance Law via Variable Structure Control," *Journal of Guidance, Control and Dynamics*, Vol. 24, No. 6, 2001.
- [13] Tal Shima, Moshe Idan and Oded M. Golan, "Sliding-Mode Control for Integrated Missile Autopilot Guidance," *Journal of Guidance, Control and Dynamics*, Vol. 29, No. 2, April 2006.
- [14] Haijun Lee, Xianlin Huang, Hang Yin, "Enhanced Sliding Mode Control for Missile Autopilot Based on Nonlinear Disturbance Observer," in *Proc. IEEE International Joint Conference on Computational Sciences and Optimization*, China.
- [15] T.W. Hwang, M. Tahk and C. Park, "Adaptive Sliding Mode Neural Net Control for Missile Autopilot," in *Proc. International Conference on Control and Automation*, Hungary, 2005, pp.26-31.
- [16] Yi-Chang Tsai and, An-Chyau Huang, "Multiple-Surface Sliding Controller Design For Pneumatic Servo Systems," *Journal of Mechatronics*, Volume. 18, 2008, pp. 506-512.
- [17] Johns Hopkins, "An Overview of Missile Flight Control Systems" (2010), *APL Technical Digest*, Volume 29, November 1, (2010).
- [18] J.H Blakelock, "Automatic Control of Aircraft and Missiles," Second Edition, Willey, NewYork, 1991.
- [19] Bernard Friedland, "Control System Design, An Introduction to State Space Methods," 2005 Edition, McGraw-Hill, Inc.
- [20] Uzair Ansari, Saqib Alam, Syed Minhaj-un-Nabi Jaffery, "Modeling and Control of Three phase BLDC Motor using PID with Genetic Algorithm," In *Proceedings of IEEE 13th International Conference on Modeling and Simulation*,UK,2011,pp. 189-194.
- [21] Binjan Bandyopadhyay, Fulwani Deepak and, Kyung-soo Kim, "Sliding Mode Control Using Novel Sliding Surfaces," *Lecture Notes In Control and Information Sciences (LNCIS)*, India.
- [22] K.D Young, V.I. Utkin and, U. Ozguner, "A Control Engineers Guide to Sliding Mode Control," *IEEE Transactions on Control Systems Technology*, Volume, 7. No 3, 1999.
- [23] Burton J.A. and, Zinober A.S.I, "Continuous Approximation of Variable Structure Control," *International Journal of Systems*, Vol.17, No. 6, pp. 875-885, 1986.

- [24] D. Swaroop, J. K. Hedrick, P.P. Yip, and, J. C. Gerdes, “Dynamic Surface Control for a Class of Nonlinear Systems,” IEEE Transactions on Automatic Control, Volume. 45, NO. 10, October 2000.
- [25] J.J.E, Slotine, Weiping Lie, “Applied Nonlinear Control,” Prentice-Hall, Inc, 1991.
- [26] V.I Utkin, J. Guldner and, J. Shi, “Sliding Mode Control in Electromechanical Systems,” Taylor and Francis, 1991.